Prepared for:

Elena McDonald-Buller
Project Manager
Texas Air Quality Research Program

Prepared by:

Jeremiah Johnson, Tejas Shah, Greg Yarwood
Ramboll
Novato, California

Daniel Goldberg, Daniel Huber
George Washington University
Washington, DC

Benjamin de Foy
Saint Louis University

September 2, 2025

AQRP Project 24-004

Evaluating Updates to CAMx and NOx Emission Inventories using TEMPO Measurements over Texas

Final Report

Contents

Tables

Figures

ACKNOWLEDGEMENT

The preparation of this report (Project No. 24-004) was funded by a grant from the Texas Air Quality Research Program (AQRP) at The University of Texas at Austin through the Texas Emission Reduction Program (TERP) and the Texas Commission on Environmental Quality (TCEQ). The findings, opinions and conclusions are the work of the authors and do not necessarily represent findings, opinions, or conclusions of the AQRP or the TCEQ.

LIST OF ACRONYMS AND ABBREVIATIONS

agl	above ground level
AMF	Air Mass Factor
AQRP	Air Quality Research Program
ARW	Advanced Research WRF
BC	Boundary Conditions
BDSNP	Berkeley-Dalhousie Soil NOx Parameterization
BVOC	Biogenic Volatile Organic Compounds
CAMPD	Clean Air Markets Program Division
CAMS	Continuous Air Monitoring Station
CAMx	Comprehensive Air quality Model with extensions
CST	Central Standard Time
DDM	Decoupled Direct Method
DFW	Dallas – Fort Worth
EBI	Euler Backward Iteration
ECMWF	European Centre for Medium-Range Weather Forecasts
EDGAR	Emissions Database for Global Atmospheric Research
EGU	Electric Generating Unit
EPA	Environmental Protection Agency
ERA5	5th generation ECMWF atmospheric reanalysis
FD	Flux divergence
FINN	Fire INventory from NCAR
FT	Free Troposphere
GCAS	GEO-CAPE Airborne Simulator
GDAS	GFS Data Assimilation System
GEOS-CF	Goddard Earth Observing System Composition Forecasting model
GFS	Global Forecasting System
HCHO	Formaldehyde
HGB	Houston-Galveston-Brazoria Area
HNO_3	Nitric acid
HONO	Nitrous acid
IC	Initial Conditions
K	Kelvin
km	kilometer
LNOx	Lightning NOx emissions
LSM	Land Surface Model
m	meter
mb	millibars
MB	Mean Bias
MDA8	maximum daily average over 8 hours
ME	Mean Error
MEGAN	Model of Emissions of Gases and Aerosols from Nature
MLR	Multiple Linear Regression
MM5	Mesoscale Model version 5
MODIS	Moderate Resolution Imaging Spectroradiometer (satellite)
MPI	Message Passage Interface
MSKF	Multi-Scale Kain-Fritsch
NAAQS	National Ambient Air Quality Standard
NASA	National Aeronautics and Space Administration

NCAR	National Center for Atmospheric Research
NMB	Normalized Mean Bias
NME	Normalized Mean Error
NO_2	Nitrogen Dioxide
NOx	Oxides of Nitrogen
OA	Organic Aerosol
OH	Hydroxyl radical
OMI	Ozone Monitoring Instrument (satellite)
OMP	Open Multi-Processing
ON	Organic Nitrate
OSAT	Ozone Source Apportionment Technology
PAN	Peroxyacyl nitrates
PBL	Planetary Boundary Layer
*p*NO3	particle nitrate photolysis
ppb	parts per billion
PSAT	Particulate Source Apportionment Technology
QA	Quality Assurance
QC	Quality Control
RFP	Reasonable Further Progress
RH	Relative Humidity
RRTMG	Rapid Radiative Transfer Model for Global applications
SAT	Source apportionment technology
SCD	Slant Column Density
SIP	State Implementation Plan (for the ozone NAAQS)
SOA	Secondary Organic Aerosol
T	Temperature
TEMPO	Tropospheric Emissions: Monitoring of POllution (satellite)
TexAER	Texas Air Emissions Repository
TexN	Texas NONROAD
TCEQ	Texas Commission on Environmental Quality
TM5	Tracer model version 5
tpd	tons per day
TRACER-AQ	Tracking Aerosol Convection ExpeRiment – Air Quality
TROPOMI	Tropospheric Monitoring Instrument (satellite)
US	United States
VIIRS	Visible Infrared Imager-Radiometer Suite (satellite)
VOC	Volatile Organic Compound
VCD	Vertical Column Density
WRF	Weather Research and Forecast model
YSU	Yonsei University

EXECUTIVE SUMMARY

Nitrogen oxide (NOx) emissions are critical to ozone formation in Texas. The research team previously demonstrated in Air Quality Research Program (AQRP) project (22-023; Goldberg et al., 2023) that highly resolved NO_2 columns (sub 1 km) can constrain the Houston NOx emission inventory with source-category specificity. However, the Comprehensive Air quality Model with extensions (CAMx) air quality model suffered a region-wide low-bias in NO_2 columns similar to biases found by other models that have been attributed to deficits in background tropospheric NO_2. Therefore, in this project several improvements were made to the NOx emission inventory and the CAMx model to reduce this low bias.

In this project, the research team tested whether NO_2 columns from the new Tropospheric Emissions: Monitoring of POllution (TEMPO) satellite can similarly constrain the Houston NOx emission inventory with source-category specificity using the ability of CAMx to tag NO_2 concentrations (and columns) by source sector. The TEMPO product has a coarser spatial resolution (2 x 4.5 km^2) than the data available to the previous work which used aircraft column NO_2 measurements at 250 x 560 m^2 spatial resolution. While TEMPO provides hourly data resolution, it was found that the monthlong modeling period was not long enough to overcome the limitations imposed partially by the coarser spatial resolution. Other issues encountered with the TEMPO product (low sun angle measurements, high albedo, cloud obscured scenes, etc.) which limited the comparison will likely improve over time.

This work mapped to three Research Priority Areas of the Texas Air Quality Research Program (AQRP), as shown in the table below.

Table 1. How this project will respond to the AQRP Research Priority Areas

Research Priority Area	How this project addresses the Research Priority
Improve accuracy of photochemical grid models	Evaluated whether adding particle nitrate photolysis (*p*NO3) in CAMx improved comparisons of modeled NO_2 to satellite NO_2 columns and near-surface measurements.
Improve emissions inventories	Improved the modeling emission inventories by adding aircraft emissions and updating the soil NOx algorithm in Model of Emissions of Gases and Aerosols from Nature (MEGAN) to adjust to soil moisture more dynamically. Evaluated NOx emission inventories using TEMPO satellite measurements by applying the flux divergence method. Tested whether TEMPO data can constrain Houston NOx emissions by source category similarly to AQRP project 22-023.
Use of satellite and other remote sensing data	Utilized TEMPO satellite to better understand diurnal patterns of NO_2 and its relationship to NOx emissions. Applied TEMPO satellite data as mentioned in the priority areas above. Tropospheric Monitoring Instrument (TROPOMI) data was also utilized in comparison to TEMPO when there was temporal overlap in the early afternoon.

This project determined how TEMPO can be used for NOx emissions evaluation. The TEMPO NO_2 measurements were used to evaluate CAMx model updates to NOx chemistry and the NOx emission inventory. Lessons learned and techniques developed for this project could be applied to other areas in the United States. The project also demonstrated the capability to estimate NOx emissions using the flux divergence method and multiple linear regression model applied to TEMPO NO_2 measurement.

This project had five tasks to accomplish the primary objective of better understanding how TEMPO could help evaluate the NOx emission inventory across Texas. The results from these five tasks are summarized here and more details are provided in Section 2.

Task 1. Texas 4-km CAMx Baseline simulation for NO_2 and Ozone

For this project, the Weather Research and Forecast (WRF) and CAMx models were run at 4 km x 4 km spatial resolution for August 25 through September 30, 2023. Anthropogenic emissions were developed from the 2019 TCEQ modeling inventory (closest to 2023 available) with addition of aircraft climb-out (above 1 km) and cruise emissions based on the Emissions Database for Global Atmospheric Research (EDGAR) 0.1° global database (Crippa et al., 2023). Lightning NOx (LNOx) emissions were developed using Ramboll's LNOx processor. Biogenic emissions were developed using the WRF simulation and MEGAN version 3.21. This version of MEGAN updates the Berkeley-Dalhousie Soil NOx Parameterization (BDSNP; Hudman et al., 2012) in MEGAN by implementing new temperature and soil moisture response functions, incorporating updated nitrogen deposition and fertilizer application data, and modeling soil nitrous acid (HONO) emissions (Ramboll 2025a; 2025b).

The near-surface Baseline CAMx model performance for Maximum Daily Average 8-hour (MDA8) ozone showed a persistent positive bias (Normalized Mean Bias [NMB]: +22.4%; Normalized Mean Error [NME]: 25.8%; mean bias: 12.1 ppb) across the CAMx 4-km domain. Performance against the NO_2 Continuous Air Monitoring Stations (CAMS) monitors showed better results than in AQRP 22-023. Across the CAMx 4-km domain, NMB was -27.8%, NME was 54.1% and the mean bias was -1.7 ppb. Examination of performance at individual sites revealed consistent underpredictions at urban and near-roadway monitors and overpredictions at monitors in rural oil and gas producing regions.

Task 2. Create TEMPO NO_2 Diurnal Profiles and Compare to Diurnal NOx Emission Maps

TEMPO NO_2 measurements were processed and averaged across a 37-day period of August 25, 2023 through September 30, 2023. In most areas, TEMPO NO_2 was largest in the morning hours (8 - 9 AM local time) decreasing until about 11 AM local time and flat throughout the rest of the day. The team re-processed the TEMPO NO_2 measurements with vertical NO_2 assumptions from CAMx and found generally minimal changes with some important exceptions. In Dallas, the operational NO_2 measurements show a large early morning spike that is not evident in the reprocessed TEMPO NO_2 measurements. In Houston, there is a temporary NO_2 peak in the mid-morning hours between 9 – 11 AM. In all areas, when using the reprocessed TEMPO NO_2 measurements, the late afternoon pattern between 3 – 6 PM local time is flatter than using the operational TEMPO NO_2 measurements. These findings underscore the enhanced uncertainties of TEMPO NO_2 in the mid-morning and late afternoon.

NOx emission maps were then created from the TEMPO NO_2 measurements directly and found that NOx emissions are generally larger in CAMx than TEMPO especially in a rural area southwest of Houston. The research team also found that TEMPO cannot capture the enhanced NOx from most point sources, although it can capture the largest point sources better than TROPOMI.

Task 3. Comparison of NO_2 Columns between CAMx and TEMPO

CAMx generally had larger simulated column NO_2 than TEMPO over most hours of the day and over most of the investigated subregions, with some important distinctions and exceptions.

The CAMx NO_2 overestimate was largest in the early morning, late afternoon, and over rural areas most associated with soil NOx and lightning NOx emissions. From this comparison, it is therefore concluded that soil NOx and lightning NOx emissions need to be further revised down. The large CAMx overestimates near daybreak and sunset could not be resolved, but this issue could result from how

the boundary layer is being resolved in the model during these hours. Future work should target these hours and rural areas.

The team also found a CAMx NO_2 underestimate that was confined to urban areas during morning hours but changed to an overestimate in the late afternoon. Future work should investigate temporal allocation of anthropogenic emission sectors, including on-road and off-road mobile and industrial emissions.

Task 4. CAMx Updates and Testing

Following the Baseline CAMx simulation and subsequent model performance evaluation (Task 1) and comparison to TEMPO NO_2 columns (Task 3), Ramboll performed a series of short CAMx sensitivity tests both with and without source apportionment to investigate changes to the MEGAN biogenic emissions, boundary conditions and a CAMx chemistry update involving organic nitrate (*p*NO3) photolysis. Ramboll considered further CAMx updates involving vertical mixing, but the evaluation of surface NO_2 performance did not suggest that vertical mixing updates would lead to improved model performance.

Ramboll updated the CAMx parametrization of organic nitrate (ON) hydrolysis (Hildebrandt Ruiz and Yarwood, 2013) to consider reaction rate dependence on the molecular mixing time within aerosol particles. As expected, this update showed near-zero impacts to surface NO_2 concentrations and only minor impacts in the free troposphere, which did not substantially change the NO_2 column amounts.

The MEGAN soil NOx emission reductions in the Final run reduce positive NO_2 biases in rural areas relative to the Baseline run. The substantial negative NO_2 biases in urban areas are made slightly larger by the soil NOx emission reductions. The positive NO_2 biases in oil and gas producing regions in the Baseline run are reduced slightly in the Final run.

During 2023, the high-sensitivity NOx instrument collected NO_2 measurements adjacent to TCEQ's NOx instrument at Tyler Airport (CAMS 82) in Northeast Texas. Ramboll compared the Baseline and Final modeled NO_2 concentrations against these "true NO_2" measurements to better understand the impact of the MEGAN soil NOx emission adjustments. The MEGAN soil NOx emission adjustments in the Final CAMx run improve the NO_2 mean bias considerably (Baseline: +0.6 ppb; Final: -0.1 ppb), while also reducing the error (Baseline NME: 44.8%; Final NME: 38.2%).

The MEGAN soil NOx emission reduction in the Final run reduces the large positive ozone bias in the Baseline run substantially. Houston, Dallas-Fort Worth and Texas all have bias and error statistics that are within or close to the Emery et al. (2017) goal benchmarks (NMB: <±5%; NME: <15%) in the Final run. San Antonio also shows a substantial reduction in ozone bias in the Final run, but performance is worse (mean bias: +5.7 ppb) than the other regions (still within criteria benchmarks).

Task 5. Estimating NOx Emissions by Sector and by Time of Day using CAMx Source Apportionment and TEMPO Retrievals

In the final task of this project, the team applied flux divergence analysis to TEMPO NO_2 retrievals over Texas—the first application of this method to TEMPO data, to the researchers' knowledge. This analysis clearly identifies cities in Texas as well large point sources. In addition, many of the highways show up as line sources using flux divergence, which is an improvement on prior results using TROPOMI retrievals (Goldberg et al., 2024a; Sun, 2022). However, data from the full data record available, from August 2, 2023 to March 31, 2025 was needed to observe these features. The team also found that retrievals before 10 AM and after 4 PM CST were less reliable due to large solar zenith angle. The quality of these retrievals could improve in future TEMPO product releases.

Finally, a multiple linear regression (MLR) model was applied together with simulated column NO_2 source apportionment information from CAMx and TEMPO NO_2 column measurements to evaluate NOx emission inventory sectors. This MLR model follows the one developed for GCAS in AQRP 22-023. In addition to configuring MLR models for the entire domain, the team applied separate MLR model simulations for three subdomains covering each of the Dallas-Fort Worth, Houston and Central Texas (includes San Antonio and Waco) regions. The model suggests that on-road mobile emissions are underestimated in Dallas-Fort Worth and East Texas overall, but Houston and Central Texas on-road mobile emissions show much better agreement (smaller underestimates) with TEMPO columns. The MLR results suggest that most other sectors need to be reduced, including lightning and soil NOx. Further evaluation of these emission sectors using CAMx together with TEMPO column measurements is suggested.

1.0 INTRODUCTION

This document provides the draft final report for the Texas Air Quality Research Program (AQRP) Project 24-004, "Evaluating Updates to CAMx and NOx Emission Inventories using TEMPO Measurements over Texas". The goal of Project 24-004 was to understand whether NO_2 columns from the TEMPO satellite can constrain the Houston NOx emissions by source sector. This project is among the first to compare TEMPO NO_2 measurements with air quality model results and evaluate how TEMPO can be used for NOx emissions evaluation.

The project Principal Investigator is Mr. Jeremiah Johnson (Ramboll). Other personnel on the project team are Dr. Daniel Goldberg (George Washington University), Dr. Greg Yarwood (Ramboll), Dr. Benjamin de Foy (Saint Louis University), and Dr. Daniel Huber (George Washington University). The AQRP project manager is Dr. Elena McDonald-Buller at the University of Texas, Austin. The project liaison for the Texas Commission on Environmental Quality (TCEQ) is Robert Keirstead.

1.1 Background

Previous studies have shown the unique benefit of using spatially continuous satellite data to evaluate NOx emissions in regional chemical transport model simulations (e.g., Canty et al., 2015; Curier et al., 2014; Harkey et al., 2015; Kemball-Cook et al., 2015; Souri et al., 2016; Travis et al., 2016). These studies compared satellite NO_2 columns to model simulations accounting for the vertical sensitivity of the satellite measurement. Results were mixed but generally found that satellite NO_2 was larger than the model in rural areas and smaller in urban areas. These studies suggested a potential overestimate of NOx emissions in U.S. urban areas and demonstrated the importance of stratospheric transport, lightning NOx emissions, soil NOx emissions, and NO_2 chemical recycling. Prior work by scientists on this team, sponsored by AQRP (project 20-020), demonstrated the capability to estimate NOx emissions for the Dallas/Fort Worth metropolitan region for the summer of 2019 using the Tropospheric Monitoring Instrument (TROPOMI; Holloway et al., 2021). Agreement between satellite and modeled column NO_2 was within 20%. In a follow-up project focused on Houston (Goldberg et al., 2023; 2024a; Nawaz et al., 2024), the team was able to gain evidence for a low bias in the satellite instrument, that led to artificial agreement between satellite and model, and therefore modeled urban NOx emissions are now biased low (a model rural low bias still persisted as with previous studies). The latter project was also able to quantify neighborhood-scale and sector-by-sector NOx emission biases using a combination of satellite data, aircraft data, and sub-kilometer chemical transport models. Outside of Texas, the team has conducted similar analyses for other North American cities (Goldberg et al., 2019a, 2019b, 2024b), power plants (de Foy et al., 2015), South Asia (de Foy and Schauer, 2022), and global megacities (Goldberg et al., 2021) using TROPOMI and a complementary satellite instrument, the Ozone Monitoring Instrument (OMI).

Comparison of satellite and modeled NO_2 columns often reveals a widespread and persistent low model bias, often attributed to the free troposphere. In this project, the research team evaluated whether TEMPO NO_2 columns can constrain NOx emissions as successfully as the Geostationary Coastal and Air Pollution Events (GEO-CAPE) Airborne Simulator (GCAS) aircraft and determined whether updates to NOx chemistry (particle nitrate photolysis) and the NOx emissions inventory in the CAMx model can improve agreement with measured NO_2 columns.

Recently, Shah et al. (2023) comprehensively evaluated free troposphere NOx (FT-NOx) measurements over the Continental United States (CONUS), agreement between the Goddard Earth Observing System with Chemistry (GEOS-chem) model and these measurements, emission source contributions to FT-NOx in GEOS-chem, the potential influence of particulate nitrate (*p*NO3) photolysis

to FT-NOx, and overall implications for comparing modeled to observed NO_2 columns. Findings of Shah et al. (2023) guide the approach outlined here to improving CAMx simulations of FT-NOx.

Figure 1.1.1, adapted from Shah et al. (2023), shows vertically resolved source contributions to NOx over the contiguous US in summer (August). Lightning and aircraft NOx emissions in the FT are important above the planetary boundary layer (PBL) and particularly important to column NO_2 measurements because instrument sensitivity is greater above the PBL. Upward transport of near-ground NOx emissions makes these emissions important throughout the tropospheric column. Ramboll (1) added aircraft emissions above 1,000 ft above ground level (agl) because they are usually omitted from regulatory modeling databases, including Texas Commission on Environmental Quality (TCEQ's) modeling platform (2) improved estimation of soil NOx emissions by updating the Berkeley-Dalhousie Soil NOx Parameterization (BDSNP; Hudman et al., 2012) algorithm in MEGAN3. Ramboll also implemented in CAMx a scheme for *p*NO3 photolysis similar to Shah et al. (2023), while preserving the integrity of the CAMx tools for source apportionment (Ozone Source Apportionment Technology and Particulate Source Apportionment Technology; OSAT and PSAT) and sensitivity analysis (Direct Decoupled Method; DDM).

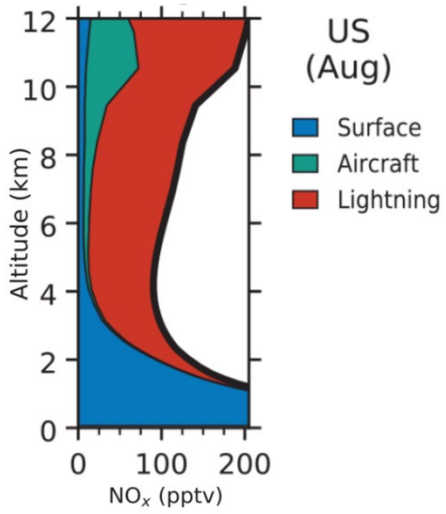

Figure 1.1.1. Vertically resolved source contributions to NOx over the contiguous US in summer modeled by GEOS-chem (adapted from Shah et al., 2023).

1.2 Overview of Approach

This project determined how TEMPO can be used for NOx emissions evaluation. TEMPO NO_2 measurements were used to evaluate CAMx model updates to NOx chemistry and the NOx emission inventory. Lessons learned and techniques developed for this project could be applied to other areas in the United States. The project also demonstrated the capability to estimate NOx emissions using the flux divergence method and multiple linear regression model applied to TEMPO NO_2 measurements.

1.3 Overview of Report

In Section 2, a comprehensive overview of the results of all five tasks of this project are provided, including CAMx simulations, emissions and satellite data processing, data comparisons, and results on emissions analysis. In Section 3, we present conclusions and recommendations for future work. Section 4 presents information about the audits of data quality.

2.0 TASK RESULTS

2.1 Texas 4-km CAMx Baseline simulation for NO_2 and Ozone

Ramboll ran WRF and CAMx with 4-km grid resolution over East Texas for August 25 – September 30, 2023 using emission inventory data from the TCEQ. TCEQ's 2019 State Implementation Plan (SIP) WRF and CAMx configurations were followed to the extent possible for consistency and to enable use of TCEQ emission data. A model performance evaluation against surface monitors is provided at the end of this section.

2.1.1 Model Configuration

2.1.1.1 WRF Model

The WRF model is a mesoscale numerical weather prediction system designed to serve both operational forecasting and atmospheric research needs (Skamarock et al., 2005, 2008). Version 4.6.0 of the Advanced Research WRF (ARW) was used in this study (Skamarock et al., 2021).

The WRF 36/12/4-km modeling domains are slightly larger than the corresponding CAMx domains (Figure 2.1.1) to avoid possible numerical artifacts near domain boundaries in WRF transferring to CAMx. The 36-km CAMx domain (red) includes all of the continental US, Mexico and large areas of Central America and Canada. The 36-km, 12-km (blue) and East Texas 4-km (green) domains are all used by the TCEQ for State Implementation Plan (SIP) modeling.

WRF physics options and data sources (Table 2.1.1) are similar to those used by the TCEQ for SIP modeling. Ramboll used 0.25° Global Forecasting System (GFS) data assimilation system (GDAS) analysis data (https://www.ncdc.noaa.gov/data-access/model-data/model-datasets/global-data-assimilation-system-gdas) as initial conditions for the WRF meteorological model. This GDAS data is also used for boundary conditions and data assimilation. Table 2.1.2 presents the vertical layer mapping table from 44 WRF layers to 30 CAMx layers. This layer mapping is from the TCEQ SIP modeling.

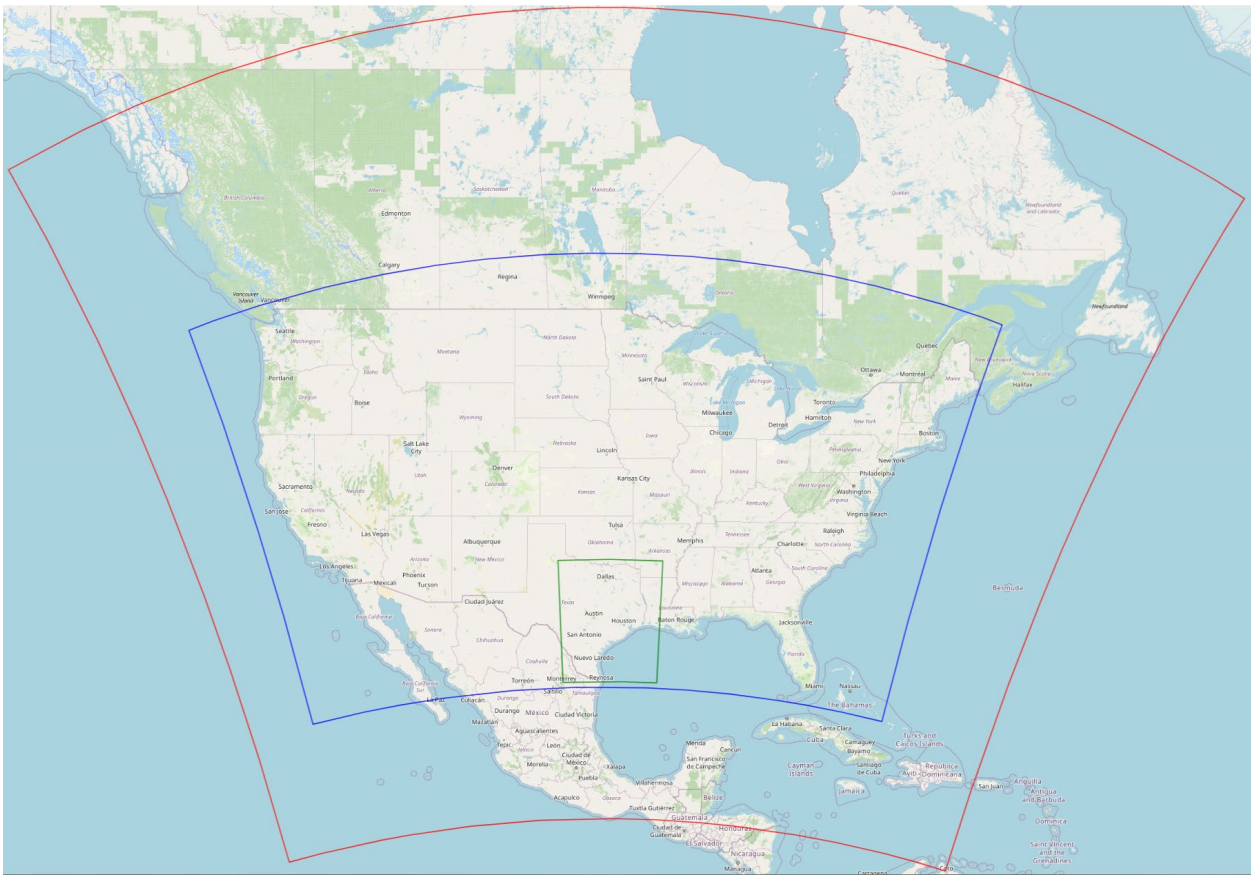

Figure 2.1.1. CAMx 36/12/4-km modeling domains.

Table 2.1.1. WRF v4.6.0 physics options and data sources used in this study.

WRF Option	Option Selected
Analysis Data	0.25° GDAS (IC/BCs and analysis nudging on the 36 and 12-km domains)
Microphysics	Thompson
Longwave Radiation	Rapid Radiative Transfer Model for Global applications (RRTMG)
Shortwave Radiation	RRTMG
Surface Layer Physics	Revised MM5 surface layer scheme
LSM	Noah
PBL scheme	Yonsei University (YSU)
Cumulus scheme	Multi-Scale Kain-Fritsch (MSKF)

Table 2.1.2. Vertical layer mapping from 44 WRF layers to 30 CAMx layers.

WRF Layer No.	WRF Eta Level	WRF Layer Pressure (mb)	WRF Layer Top (m)	CAMx Layer No.	CAMx Layer Top (m)	CAMx Layer Thickness (m)
44	0.000	50.00	20576			
43	0.010	59.63	19458			
42	0.025	74.08	18082	30	18082	3885
41	0.045	93.35	16616			
40	0.065	112.61	15427			
39	0.090	136.69	14198	29	14198	2977
38	0.115	160.77	13169			
37	0.145	189.67	12120			
36	0.175	218.57	11221	28	11221	1850
35	0.210	252.28	10304			
34	0.250	290.81	9372	27	9372	1599
33	0.290	329.34	8534			
32	0.330	367.87	7773	26	7773	1269
31	0.370	406.40	7073			
30	0.405	440.12	6504	25	6504	1040
29	0.440	473.83	5969			
28	0.475	507.54	5464	24	5464	870
27	0.510	541.26	4985			
26	0.540	570.16	4594	23	4594	737
25	0.570	599.05	4219			
24	0.600	627.95	3857	22	3857	684
23	0.630	656.85	3509			
22	0.660	685.75	3174	21	3174	325
21	0.690	714.64	2849	20	2849	314
20	0.720	743.54	2535	19	2535	304
19	0.750	772.44	2231	18	2231	247
18	0.775	796.52	1984	17	1984	241
17	0.800	820.60	1744	16	1744	235
16	0.825	844.68	1509	15	1509	230
15	0.850	868.76	1279	14	1279	135
14	0.865	883.21	1144	13	1144	134
13	0.880	897.66	1010	12	1010	132
12	0.895	912.11	878	11	878	130
11	0.910	926.56	748	10	748	86
10	0.920	936.19	662	9	662	85
9	0.930	945.82	577	8	577	84
8	0.940	955.46	493	7	493	84
7	0.950	965.09	409	6	409	83
6	0.960	974.72	326	5	326	82
5	0.970	984.35	243	4	243	82
4	0.980	993.99	162	3	162	81
3	0.990	1003.62	81	2	81	48
2	0.996	1009.40	32	1	32	32
1	0.998	1011.32	16			
surface	1.000	1013.25	0	0	0	

2.1.1.2 CAMx Model

The science options for the CAMx simulation (Table 2.1.3) are similar to the TCEQ's SIP modeling. CAMx v7.31 was used with the CB6r5 chemical mechanism.

Table 2.1.3. Science options used for CAMx modeling.

Science Options	CAMx Configuration
Version	Version 7.31
Time Zone	CST
Vertical Grid Mesh	30 Layers with 32 m deep surface layer and 15 layers in the lowest 1.5 km
Horizontal Grids	36/12/4-km 2-way nested grids
Meteorology	2023 WRF meteorology
Chemistry Mechanism	CB6r5 gas-phase mechanism
Chemistry Solver	EBI
Probing Tool	Ozone Source Apportionment Technology (OSAT)
Photolysis Rates	TUV version 4.8 with TOMS ozone column adjustment and in-line adjustment for clouds
Advection Scheme	Piecewise Parabolic Method (PPM)
Planetary Boundary Layer (PBL) mixing	K-theory
In-line Ix Emissions On	Inorganic iodine (Ix) emissions from saltwater areas
Parallelization	MPI (18 threads) and OMP (6 threads)

CAMx NO_2 Source Apportionment Configuration

The CAMx OSAT source apportionment tool was used to track NO_2 from 8 sectors (Table 2.1.4). All remaining NOx emissions were tracked together in the Other category.

Table 2.1.4. CAMx Source Apportionment configuration.

No.	Source Sector	No.	Source Sector
1	Biogenic (soil NOx)	5	Off-road mobile including shipping
2	Lightning NOx	6	Electric Generating Units (EGUs)
3	Aircraft climb-out and cruise	7	Oil and Gas
4	On-road mobile	8	Other

Modeling Emissions Inventory

Table 2.1.5 summarizes NOx and VOC emissions for a September weekday across the East Texas CAMx 4-km domain for the same source sectors as in Table 2.1.4 for the Baseline CAMx simulation. A pie chart shows the same values in Figure 2.1.2. For comparison, a similar pie chart is shown for the Final CAMx simulation in Figure 2.1.3. The only emissions change between the two simulations relates to soil NOx emission updates that are described later in this section.

Table 2.1.5. CAMx 4-km domain-wide summary of a September weekday emissions (tons per day) by sector for Baseline CAMx simulation.

Emission Sector	NOx (tpd)	VOC (tpd)
Biogenic	3,836	22,383
Lightning NOx	2,569	0
Aircraft climb-out and cruise	63	1
On-road mobile	645	235
Off-road mobile (incl. shipping)	527	194
EGUs	285	8
Oil and Gas	457	1,620
Other	865	2,475

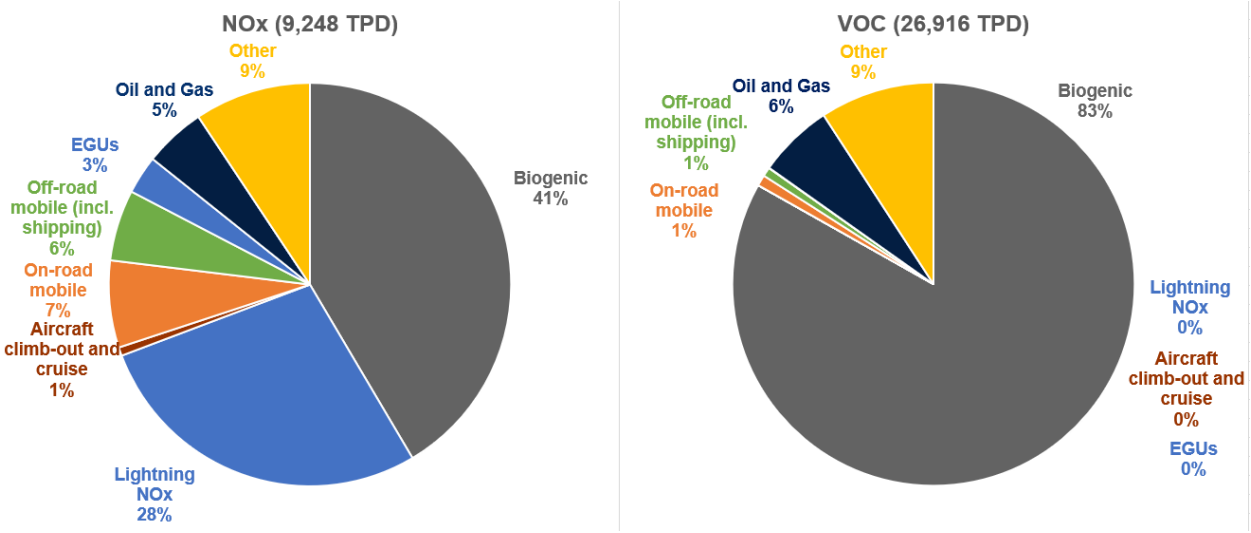

Figure 2.1.2 Pie charts of NOx and VOC emissions summaries for Baseline CAMx simulation presented in Table 2.1.5.

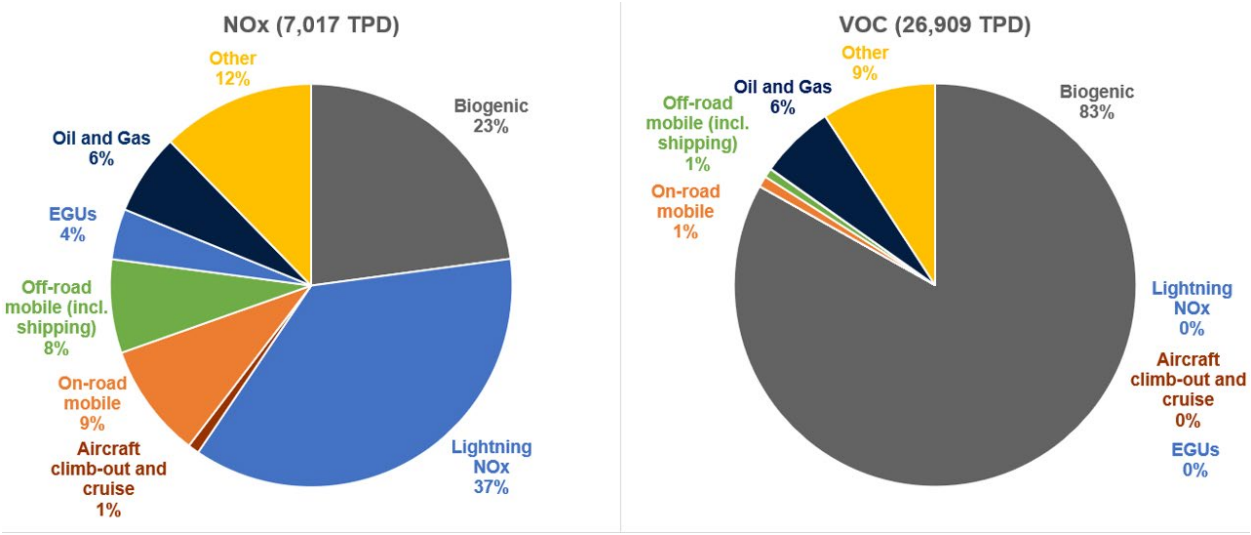

Figure 2.1.3. Pie charts of NOx and VOC emissions summaries for Final CAMx simulation.

Anthropogenic Emissions Inventory

TCEQ developed the 2019 modeling emissions inventory for the Dallas-Fort Worth (DFW) and Houston-Galveston-Brazoria (HGB) Reasonable Further Progress (RFP) SIP revision. Table 2.1.6 identifies data sources used in this inventory. These tables are adapted from TCEQ's HGB and DFW RFP SIP revision. The changes that implemented for this study are:

- Added aircraft climb-out (above 1 km) and cruise emissions based on the Emissions Database for Global Atmospheric Research (EDGAR) 0.1° global database (Crippa et al., 2023).
- Used 2023 WRF meteorology for lightning NOx
- Used MEGAN v3.2.1 for biogenic emissions described in next section

Table 2.1.6. Data sources for emissions inventory. Adapted from Table 3-4 of TCEQ's HGB and DFW RFP SIP Revision.

EI Source Category	Sector/Geographic area	Datasets/Models used for 2019 EI
Point	EGU	2019 CAMPD
Point	Non-EGU, Texas	2019 State of Texas Air Reporting System
Point	Non-EGU, Non-Texas	EPA 2016v1 Modeling Platform
Non-Point	Oil & Gas, Texas	2019 Railroad Commission of Texas
Non-Point	Oil & Gas, Non-Texas	EPA 2017 Modeling Platform
Non-Point	Off-Shore	2017 Bureau of Ocean Energy Management
Mobile	On-Road, Texas non-attainment areas	Motor Vehicle Emission Simulator (MOVES3) - link-based
Mobile	On-Road, other	MOVES3 - county based
Mobile	Non-Road, Texas	TexN2.2
Mobile	Non-Road, Non-Texas	MOVES3
Mobile	Off-Road Shipping, 4-km domain	2019 Automatic Identification System and vessel characteristic IHS 2020; MARINER v1
Mobile	Off-Road Shipping, 12-km domain	EPA 2016v1 Modeling Platform
Mobile	Off-Road Airports, Texas non-attainment areas	Texas Transportation Institute (TTI) 2020 data
Mobile	Off-Road Airports, other	EPA 2016v1 Modeling Platform
Mobile	Off-Road Locomotives, Texas nonattainment areas	TTI 2019 data
Mobile	Off-Road Locomotives, other	EPA 2016v1 Modeling Platform
Area	Area, Texas	2020 Air Emissions Reporting Requirements
Area	Area, Non-Texas	EPA 2017 Modeling Platform
Other	International EI	2019 Community Emission Data System; SMOKEv4.7_CEDS
Natural	Biogenic	MEGAN3.2.1 using 2023 WRF meteorology
Natural	Lightning NOx	Using 2023 WRF meteorology
Natural	Fires	2019 MODIS and VIIRS; FINN v2.2

MEGAN Biogenic Emissions

The soil NOx emissions estimates were improved by updating the MEGAN3.2 model with new input data and algorithm enhancements. The Berkeley-Dalhousie Soil NOx Parameterization (BDSNP; Hudman et al., 2012), which is widely used to estimate soil NO emissions, is implemented into the Model of Emissions of Gases and Aerosols from Nature version 3.2 (MEGAN3.2). The BDSNP implementation in MEGAN was enhanced by implementing new temperature and soil moisture response functions, incorporating updated nitrogen deposition and fertilizer application data, and modeling soil nitrous acid (HONO) emissions. These updates have been integrated into the new version, MEGAN v3.21 (Ramboll 2025a, 2025b).

Our initial application of MEGAN v3.21 for the Texas 4-km domain showed that soil NOx emissions were somewhat overestimated compared to satellite-based NO_2 observations. To address this, several adjustments to the MEGAN model were implemented:

- Used soil temperature and moisture from Layer 2 for inputs to MEGAN.
- Shortened the decay period for available soil nitrogen from fertilizer from 4 to 2 months and reduced the nitrogen deposition half-life from 6 to 3 months.
- Applied a reduction factor to HONO emissions to account for soil nitrogen availability, similar to the approach used for soil NO emissions.

Table 2.1.7 compares soil NOx and Biogenic Volatile Organic Compounds (BVOC) emissions within the Texas 4-km domain as estimated by the initial MEGAN v3.21 and the updated model. Figure 2.1.4 shows the spatial distribution of soil NOx emissions across the same domain, highlighting differences between the original and updated model estimates.

Table 2.1.7. Comparison of MEGAN v3.21 and Updated Episode Average Emissions for the Texas 4-km Domain

Species	MEGAN3.21 (tpd)	MEGAN3.21 with AQRP Updates (tpd)	% Change
BVOC	21,797	21,848	0%
NOx (NO+HONO)	4,339	1,830	-58%

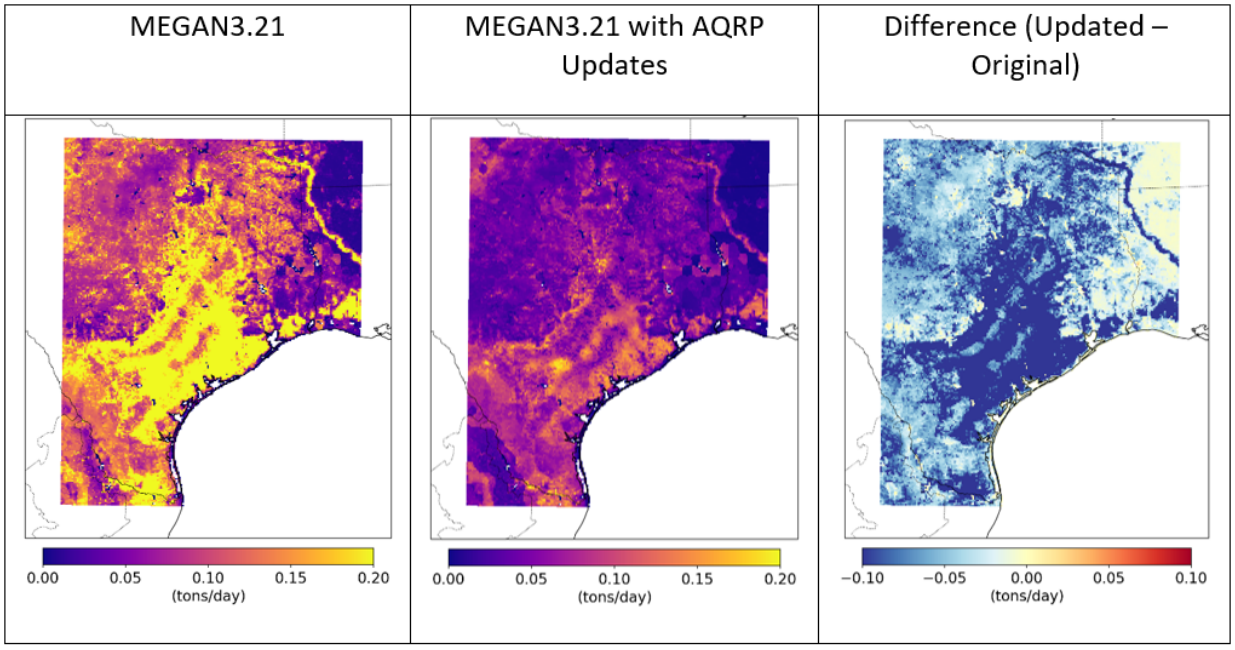

Figure 2.1.4. Spatial distribution of episode average daily soil NOx emissions in the Texas 4-km domain, estimated using MEGAN v3.21 and the updated model with AQRP revisions.

Other Natural Emissions

TCEQ estimated fire emissions from Fire INventory of NCAR (FINN) version 2.2 (Wiedinmyer et al., 2011). Ramboll developed lightning NOx emissions with the CAMx LNOx processor[1] using the 2023 WRF meteorological data.

2.1.2 Near-Surface Model Performance Evaluation

Baseline CAMx NO_2 and ozone surface concentrations were evaluated using data collected at TCEQ Continuous Air Monitoring Stations (CAMS) at all Texas CAMS within the 4-km CAMx domain. NOx monitors deployed for routine monitoring, e.g., at TCEQ CAMS, have limitations for NO_2. These monitors measure NO and consequently NO_2 is chemically converted to NO for measurement. The converter in these instruments could potentially capture other compounds including peroxyacyl nitrate (PAN) and a portion of nitric acid (HNO_3). Previous work (UH and Ramboll, 2021) comparing measurements from a high-sensitivity NOx instrument with photolytic converter (no interference of other species with NO_2) adjacent to TCEQ's NOx instrument at Tyler Airport (CAMS 82) in Northeast Texas found no evidence for substantial interference from these compounds. However, the AQRP 22-023 study found that routinely operated NOx monitors can display considerable noise below about 5 ppb. For this study, a cut-off value of 1 ppb was applied, consistent with AQRP 22-023.

The scatter plot in Figure 2.1.5 shows hourly (7 AM-5 PM CST to correspond with TEMPO availability) measurements and model pollutant concentrations at all TCEQ CAMS located within the CAMx 4-km domain (top left), Houston (top right), Dallas-Fort Worth (bottom left), and San Antonio (bottom right). Overall, the model displays a small negative NO_2 bias (mean bias, MB: -1.7 ppb; normalized mean bias, NMB: -27.8%) that is more pronounced when monitored NO_2 is low during midday. The smallest NO_2 bias of the three regions is in Houston, where the MB is -0.4 ppb and the NMB is -6.3%.

Figure 2.1.6 shows maps of the mean observed concentrations (top panel) and CAMx mean bias (bottom panel) across the entire modeling episode at each TCEQ CAMS NO_2 monitor. CAMx shows a negative NO_2 bias in urban and near roadway locations, but monitors in away from these areas show positive NO_2 biases. This pattern explains the large discrepancy in the NMB and NME values, particularly in Houston (NMB: -6.3%; NME: 50.1%). CAMx also shows positive NO_2 biases in oil and gas producing regions, including Karnes County (C1070; MB: +7.2 ppb) in the Eagle Ford Shale region.

[1] Available at https://www.camx.com/download/support-software/

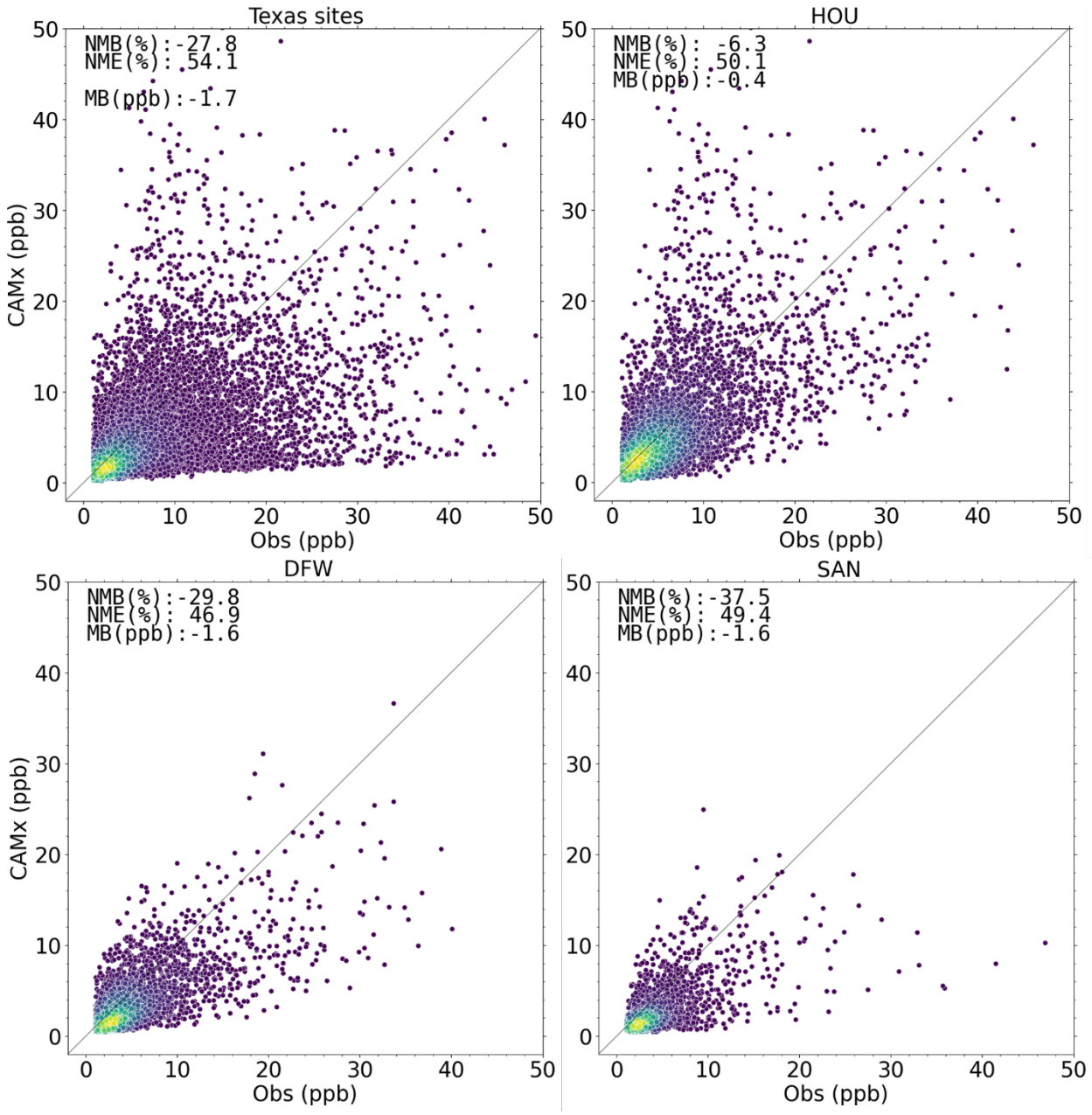

Figure 2.1.5. Hourly CAMx (7 AM-5 PM CST) NO_2 plotted against observed NO_2 across all TCEQ CAMS within Texas (top left), Houston (top right), Dallas-Fort Worth (bottom left), and San Antonio (bottom right) during the August 25-September 30, 2023 modeling period.

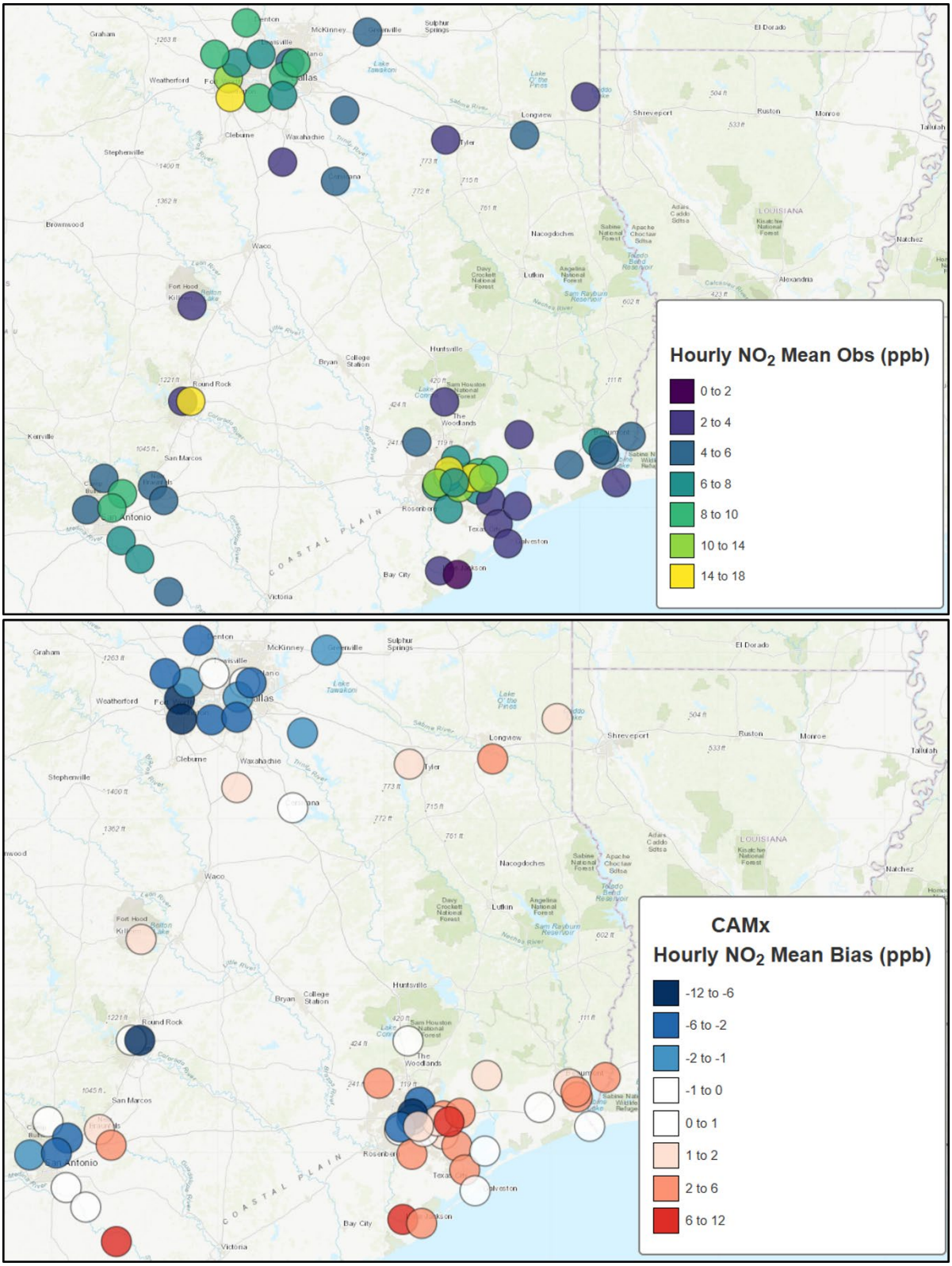

Figure 2.1.6. 7 AM-5 PM CST observed mean NO_2 (top) and CAMx NO_2 mean bias (bottom) at each TCEQ CAMS site averaged over the August 25-September 30, 2023 modeling period.

Figure 2.1.7 displays a similar scatter plot for CAMx maximum daily 8-hour average (MDA8) ozone compared to ozone observations at all CAMS in the CAMx 4-km domain (top left), Houston (top right), Dallas-Fort Worth (bottom left), and San Antonio (bottom right) in Figure 2.4. CAMx displays a persistent positive bias across the range of observed ozone concentrations. Emery et al. (2017) defines the goal benchmark for MDA8 ozone as ± 5% for normalized mean bias (NMB) and < 15% for normalized mean error (NME). The criteria (less stringent) benchmark for MDA8 ozone is ± 15% for NMB and < 25% for NME. Across Texas, CAMx achieves the criteria benchmark for NME (24.8%), while the NMB (22.4%) is outside the criteria benchmark. Section 2.4 describes the sensitivity tests conducted to identify what causes the positive ozone bias and presents the Final CAMx configuration that reduces this bias.

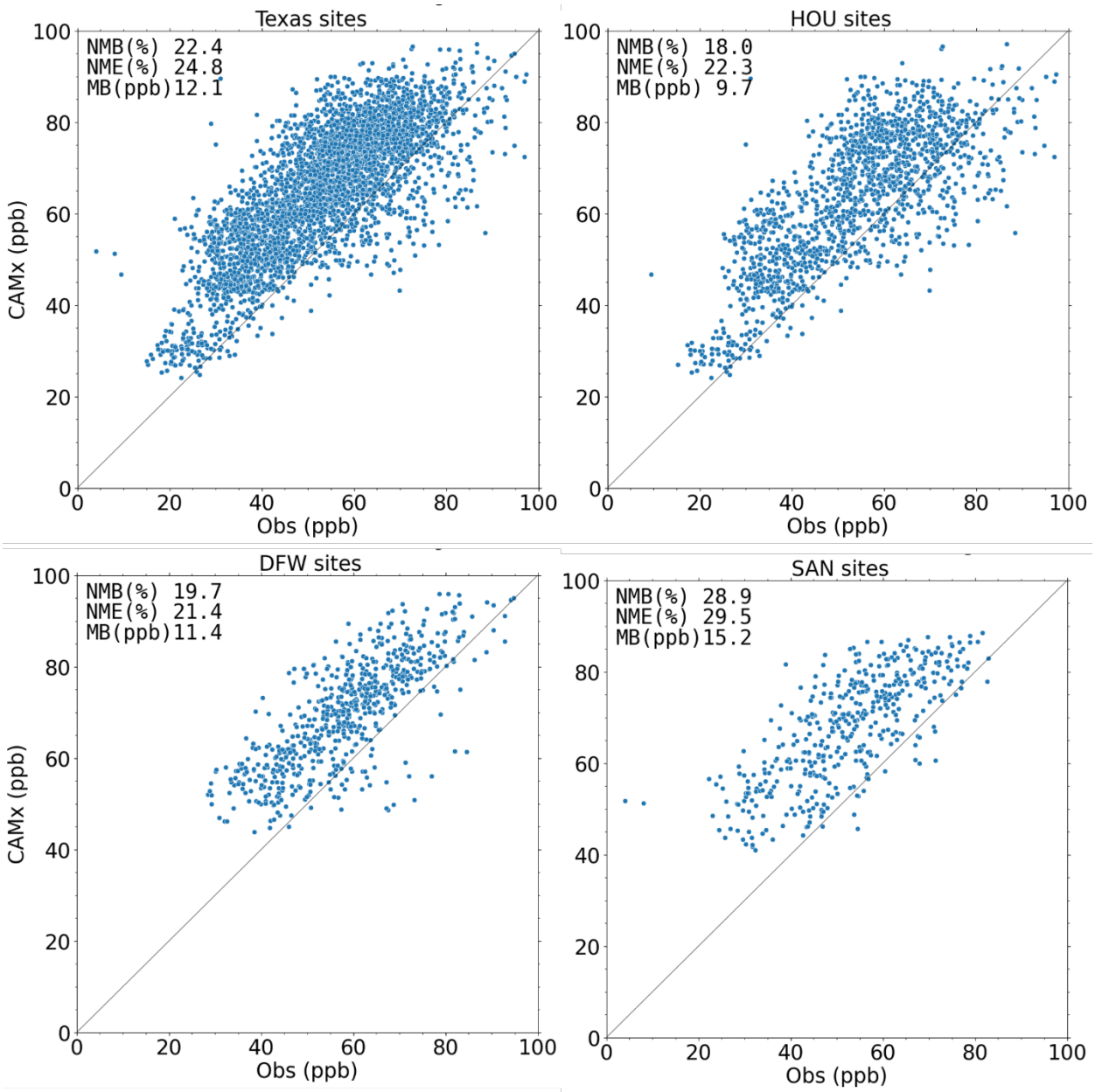

Figure 2.1.7. CAMx and observed MDA8 ozone across all TCEQ CAMS sites within Texas (top left), Houston (top right), Dallas-Fort Worth (bottom left), and San Antonio (bottom right) during the August 25-September 30, 2023 modeling period.

2.2 Create TEMPO NO_2 Diurnal Profiles and Compare to Diurnal NOx Emission Maps

TEMPO is the first remote sensing instrument to continuously gather information on column NO_2 during all daylight hours over the continental United States. Before 2023, low earth orbiting instruments, such as OMI and TROPOMI, were able to gather column NO_2 information only in the early afternoon. Prior remote sensing instruments were informative, but assumptions were needed to translate the early afternoon measurement to a different hour of the day for a full-day average.

For this task, TEMPO column NO_2 data was processed to the 4 km × 4 km CAMx grid and plotted the diurnal NO_2 patterns during August 25 – September 30, 2023 corresponding to the CAMx simulation (Figure 2.2.1). During this 37-day period there were, on average, 14 TEMPO NO_2 observations per day (~500 observations total), with only one day completely missing (September 8th) and sporadic missing hourly observations. The September 2023 timeframe also had several instances of TEMPO "special operations" (more frequent scans) over eastern Texas when there were up to 35 scans per day. These special operations occurred on September 11 – 12, 2023 and September 17 – 19, 2023, and instead of one TEMPO measurement per hour, there were five measurements per hour for several mid-afternoon hours.

Figure 2.2.1 and Figure 2.2.2 demonstrate the diurnal TEMPO column NO_2 patterns over the full CAMx model domain. Over the entire modelling period, average column NO_2 is 1.29× larger in the mid-morning (~9:30 AM local time) than the early afternoon. In the late afternoon (~4:30 PM local time), average column NO_2 is roughly equivalent to the early afternoon measurement. Although column NO_2 is generally larger in the morning and roughly constant throughout the afternoon, there are some exceptions to this rule, such as locations affected by sea breezes, which show continued NO_2 drops throughout the afternoon. A comparison of TEMPO and CAMx column NO_2 is presented in Section 2.3.

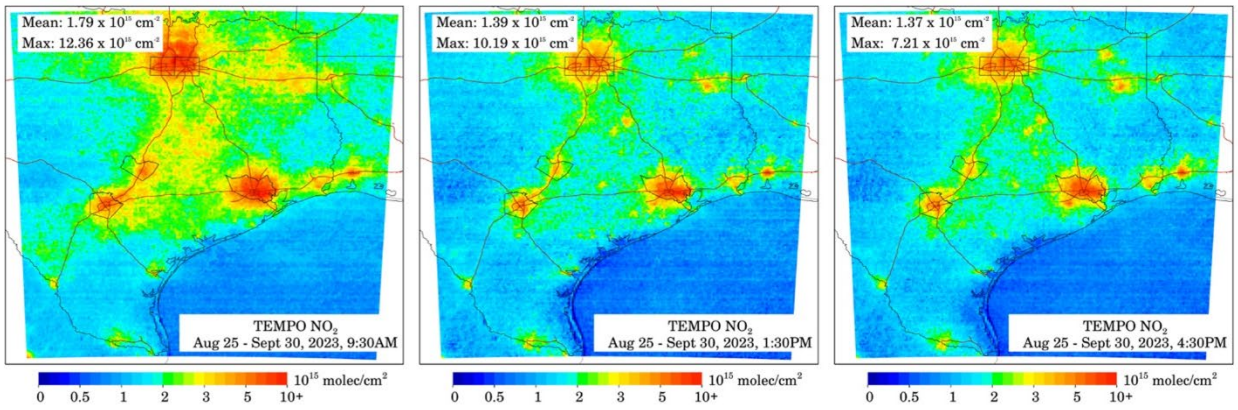

Figure 2.2.1. TEMPO NO_2 measurements averaged for the 37-day period between August 25, 2023 and September 30, 2023 at (Left) 9:30 AM local time, (Center) 1:30 PM local time, and (Right) 4:30 PM local time.

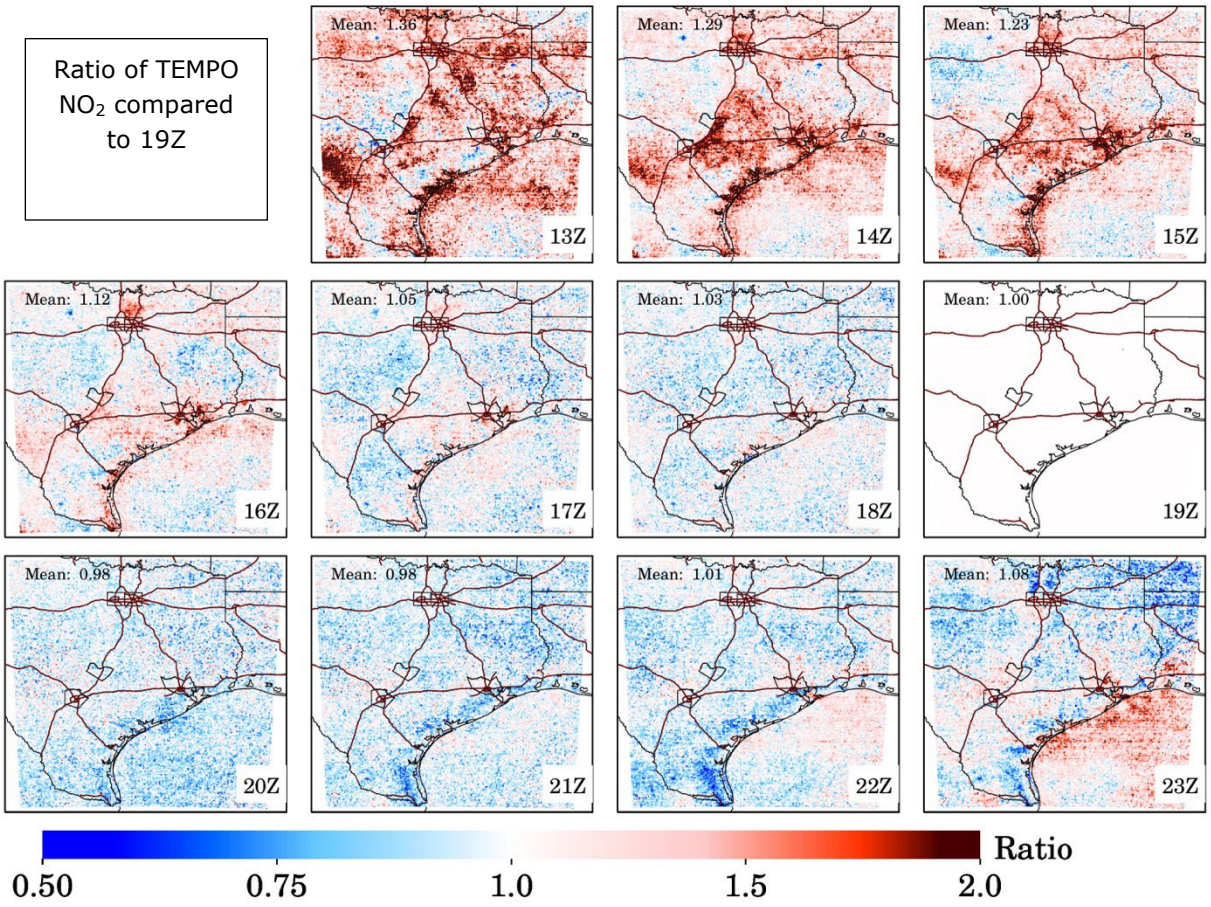

Figure 2.2.2. An average of TEMPO NO_2 at each individual hour compared to the 19Z TEMPO NO_2 measurement which is the typical TROPOMI overpass time. TEMPO NO_2 measurements are averaged for the 37-day period between August 25, 2023 and September 30, 2023.

A similar analysis of the diurnal NO_2 patterns was then conducted, now focused on eight subregions within the east Texas CAMx model domain: Austin, Dallas, Houston, San Antonio, an area in Northeast Texas (NE_TX), an area in West Texas (W_TX), an area in Deep East Texas (DeepE_TX) and a rural area between Houston and San Antonio (SE_TX). Spatial extents are shown in Figure 2.2.3. For this analysis, two additional TEMPO products are displayed, which are column NO_2 amounts processed with *a priori* vertical NO_2 profile assumptions from the two CAMx simulations, hereafter referred to TEMPO NO_2 CAMx_AMF and TEMPO NO_2 Updated CAMx_AMF.

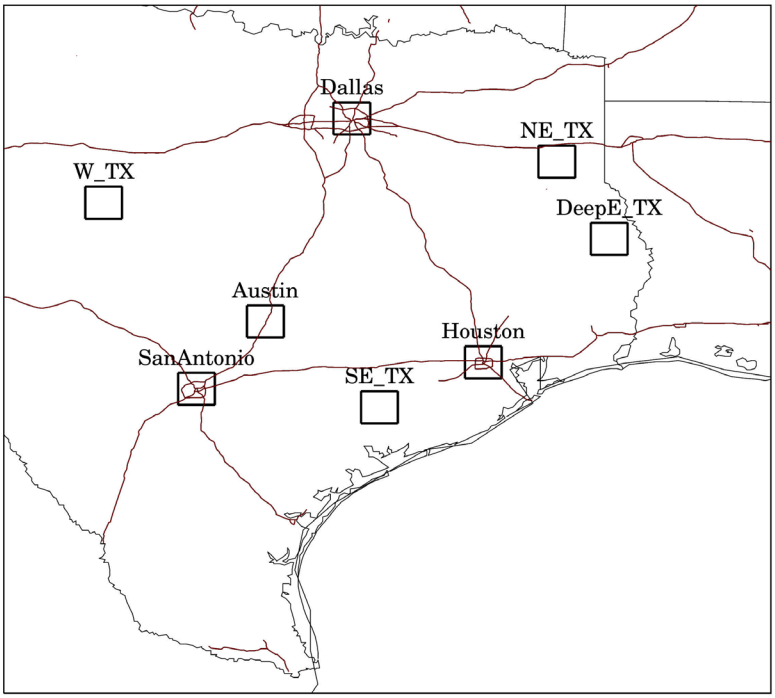

Figure 2.2.3 The eight sub-regions of interest and their spatial extents.

In all eight focus regions (Figure 2.2.4) a similar diurnal NO_2 pattern as the broad regional pattern (Figure 2.2.2) is found: NO_2 is larger in the morning than early afternoon and flattens in the afternoon. However, there are some exceptions: 1) In Dallas, the operational NO_2 measurements show a very large NO_2 spike in the early AM that is not evident when using the TEMPO NO_2 CAMx_AMF measurements; 2) In Houston, there is a notable increase in NO_2, especially in the TEMPO NO_2 CAMx_AMF measurements, in the mid-morning hours between 9 – 11 AM; 3) In DeepE_TX, the NO_2 is relatively flat through the entire day, perhaps a result of transport patterns enhancing afternoon NO_2; 4) In all areas, when using the TEMPO NO_2 CAMx_AMF measurements, the late afternoon pattern between 3 – 6 PM local time is flatter than using the operational TEMPO NO_2 measurements.

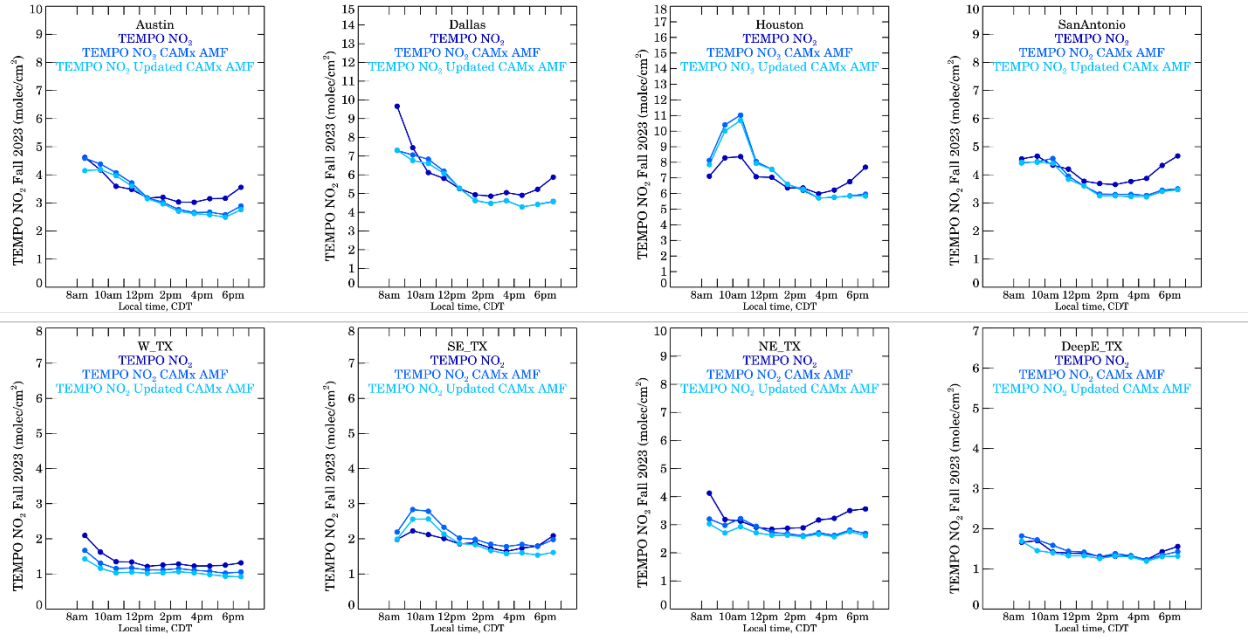

Figure 2.2.4. An average of TEMPO NO_2 at each individual hour compared for eight sub-regions denoted in Figure 2.2.3. Column NO_2 processed with a priori vertical NO_2 profile assumptions from the two CAMx simulations are shown as TEMPO NO_2 CAMx_AMF and TEMPO NO_2 Updated CAMx_AMF. All TEMPO NO_2 measurements are averaged for the 37-day period between August 25, 2023 and September 30, 2023.

In Figure 2.2.5 (TEMPO NO_2 column measurements and NOx emissions by sector for Dallas), it is demonstrated that the column NO_2 patterns are much different than the NOx emission patterns. The TEMPO column NO_2 shows a peak in the morning followed by a flattening in the afternoon (similar to results mentioned above), however, the total NOx emissions are simulated to peak in the late afternoon (3:30 PM local time) with above mean 24-hour NOx emission rates between 6:30 AM – 6:30 PM local time.

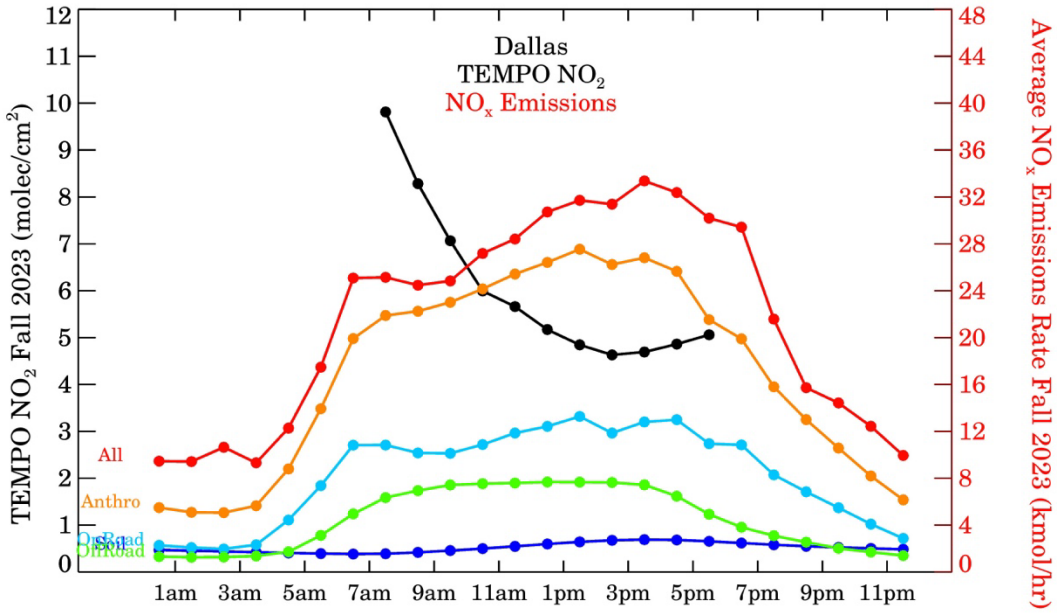

Figure 2.2.5. TEMPO NO_2 column versus NOx emission diurnal profiles

Additional variables are then processed to convert diurnal TEMPO column NO_2 patterns into diurnal NOx emissions patterns. For this, a mass conservation equation is used to calculate NOx emissions as the sum of NO_2 consumption and NO_2 accumulation between two hourly TEMPO NO_2 measurements. The consumption is denoted as the exponential decay of the average NO_2 within a given hour, whereas the accumulation is a difference between the two hourly measurements.

$$Emissions = Consumption + Accumulation$$

$$Emissions = \left[\frac{\left(NO_{2,i+1} + NO_{2,i}\right)}{2} \times \left(1 - e^{-1/\tau}\right)\right] + \left(NO_{2,i+1} - NO_{2,i}\right)$$

Finally, the NO_2 is multiplied by a NOx/NO_2 ratio of 1.32, consistent with the photochemical steady state assumption of NO_2 during daytime.

There are two major assumptions in this method: 1) mean horizontal transport equals zero during the hour; this assumption is invalid over a single day with moderate winds, however over many days, changing wind directions and speed often do lead to small mean net horizontal transport. 2) A lifetime is needed to be assumed at each hour to calculate the emissions; uncertainties in the assumed lifetime can be large (>100%) and therefore the total uncertainty can be asymptotic at short NO_2 lifetimes. The goal of this task is to develop a method to generate ***qualitative*** diurnal NOx emissions patterns without the use of a chemical transport model that could then be used to evaluate diurnal patterns assumptions of NOx emissions input into chemical transport models such as CAMx. This simple model achieves this goal. However, since the NO_2 lifetime is very uncertain, the quantitative results should be treated with caution.

In Figure 2.2.6, the TEMPO NOx versus CAMx NOx emission patterns and magnitudes is shown. Generally, there is good spatial agreement. To infer NOx emissions, a NO_2 lifetime needs to be assumed: at 10 AM a 3-hour lifetime is assumed, at 2 PM a 1.5-hour lifetime is assumed, and 5 PM a 1.5-hour lifetime is assumed. If a longer lifetime is assumed at any hour the calculated NOx emissions would be smaller, and if a shorter lifetime is assumed the calculated NOx emissions would be larger. *Therefore, the results presented here have large uncertainties and over-interpreting the quantitative comparison is not recommended.* Nonetheless, in this qualitative analysis, CAMx NOx emissions are typically larger than derived TEMPO NOx emissions over much of the domain. This disagreement may be caused by errors in both products. For TEMPO, it cannot capture the full magnitude of NOx emissions from narrow plume point sources; it can capture some of the largest point sources such as Martin Lake and W.A. Parrish, but even these sources show underestimates. For CAMx, it is likely that biogenic NOx emissions, especially southwest of Houston, are too large.

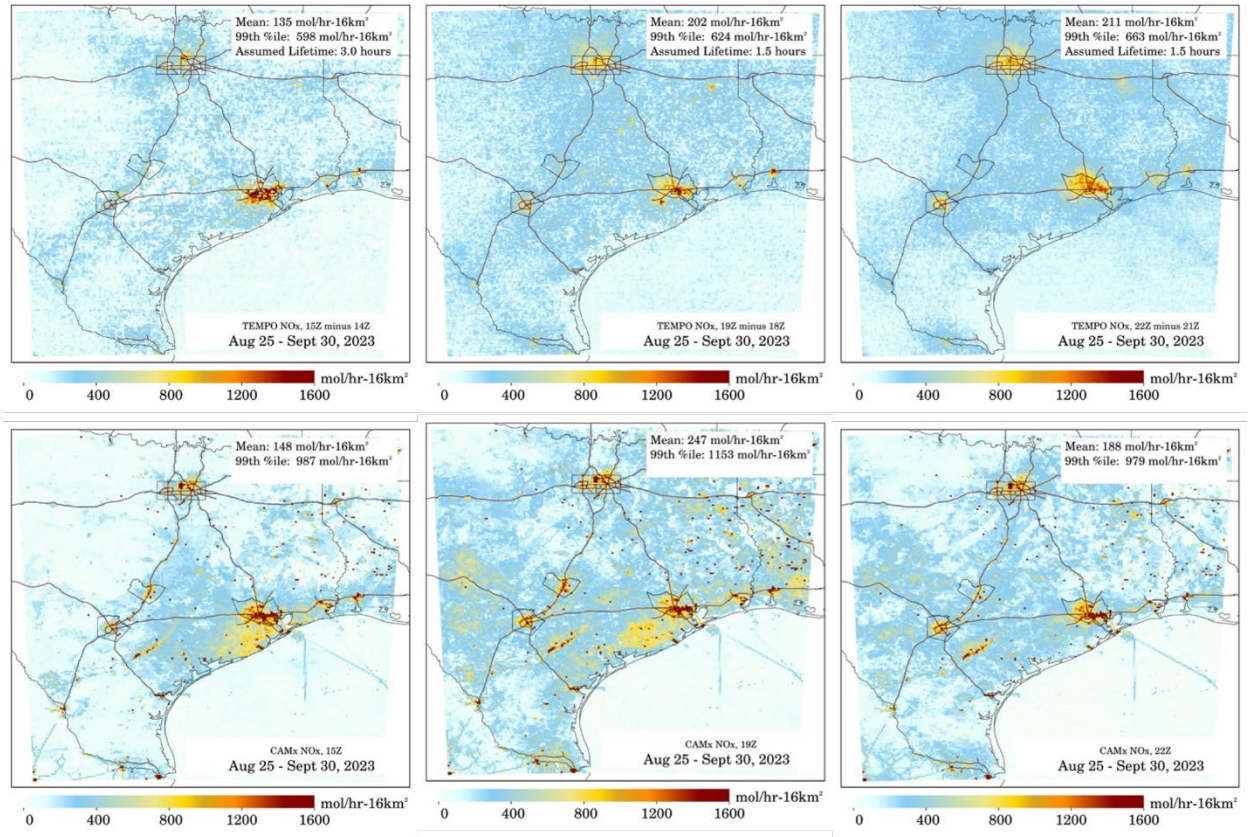

Figure 2.2.6. Top row: Calculated NOx from TEMPO at three hours: 10 AM, 2 PM, and 5 PM local time. Bottom row: CAMx NOx emissions at the same three hours.

2.3 Comparison of NO_2 Columns between CAMx and TEMPO

For this task, the team re-gridded TROPOMI NO_2 and TEMPO NO_2 columns onto the CAMx 4-km grid and re-calculated the NO_2 vertical columns of the satellite measurements using the simulated NO_2 column information from the CAMx simulation. Once re-gridded to the CAMx 4-km grid, the data can be averaged over multiple days to obtain gridded TROPOMI and TEMPO NO_2 averages when measurements are available (1 PM CST for TROPOMI, 6 AM – 5 PM CST for TEMPO).

As a prerequisite to this analysis, the satellite observations are processed using the NO_2 vertical profile information from CAMx. Without this step, satellite observations would be subject to artifacts related to their original a priori assumptions provided by the global models used to originally process them. TROPOMI uses the Tracer model version 5 (TM5), and TEMPO uses the Goddard Earth Observing System Composition Forecasting model (GEOS-CF) for TEMPO. After this re-processing is completed, it is appropriate to directly compare NO_2 columns from model and satellite to each other.

In a first comparison, Figure 2.3.1, the TROPOMI NO_2 and TEMPO NO_2 operational products are intercompared during August 25, 2023 – September 30, 2023. Generally, TEMPO NO_2 shows 25 – 50% smaller NO_2 than TROPOMI along the Texas coastline. Conversely, urban NO_2 is 10 – 30% larger in TEMPO than TROPOMI in the Texas urban areas. The mean difference of TEMPO is 7% smaller NO_2 across the full model domain.

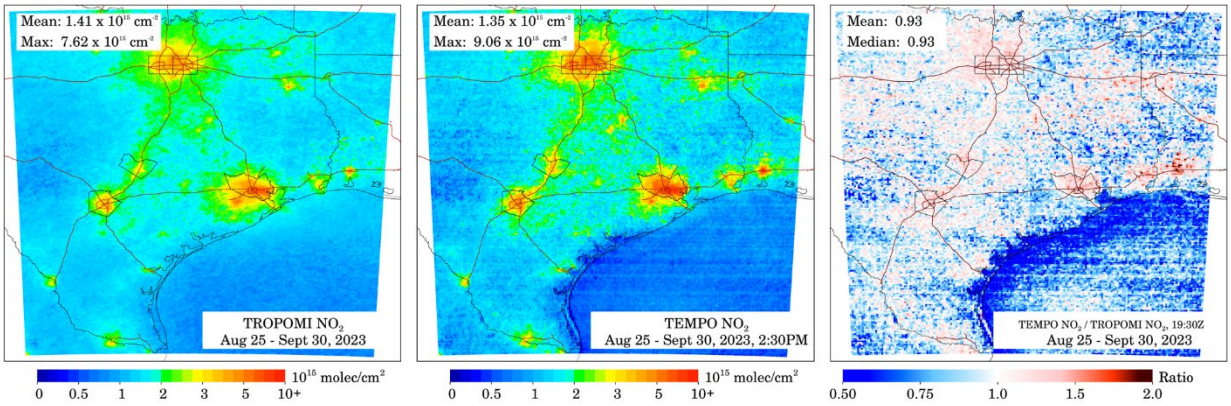

Figure 2.3.1. TROPOMI (left) and TEMPO (center) NO_2 column amounts at at 19:30Z (2:30 PM local time). Right panel shows ratio between TEMPO NO_2 and TROPOMI NO_2 column amounts.

Next both satellite measurments are re-processed with CAMx NO_2 vertical profile information, and then do the same comparison (see Figure 2.3.2). This isolates how much of the difference results from surface reflectivity and cloud assumptions as opposed to assumptions about the NO_2 vertical profile. In this comparison, similar regional patterns are displayed, but these patterns are somewhat muted. TEMPO NO_2 shows 20 – 40% smaller NO_2 than TROPOMI along the Texas coastline. Conversely, urban NO_2 is 5 – 20% larger in TEMPO than TROPOMI in the Texas urban areas. The mean difference of TEMPO is 5% smaller NO_2 across the full model domain.

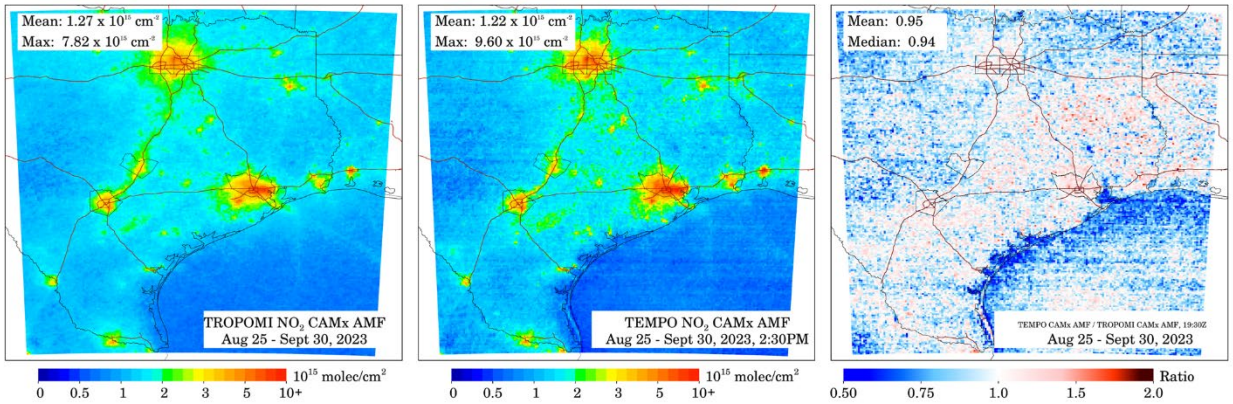

Figure 2.3.2. NO_2 column amounts using CAMx AMF for TROPOMI (left) and TEMPO (center) at 19:30Z (2:30 PM local time). Right panel shows ratio between TEMPO and TROPOMI NO_2 column amounts.

Next, TEMPO is intercompared to itself with and without CAMx NO_2 vertical profile information ingested. Figure 2.3.3 shows that CAMx information tends to drive the TEMPO NO_2 values lower by 7 – 21% depending on the hour. In the early morning (8 AM local time) and evening (6 PM local time), adjustments are largest. In urban areas, especially Houston, the CAMx information causes TEMPO NO_2 to adjust upward. The adjustment of rural values smaller and urban values larger is consistent with previous studies (Goldberg et al., 2022). However, the changes in the early morning and evening were surprising and larger than had been anticipated.

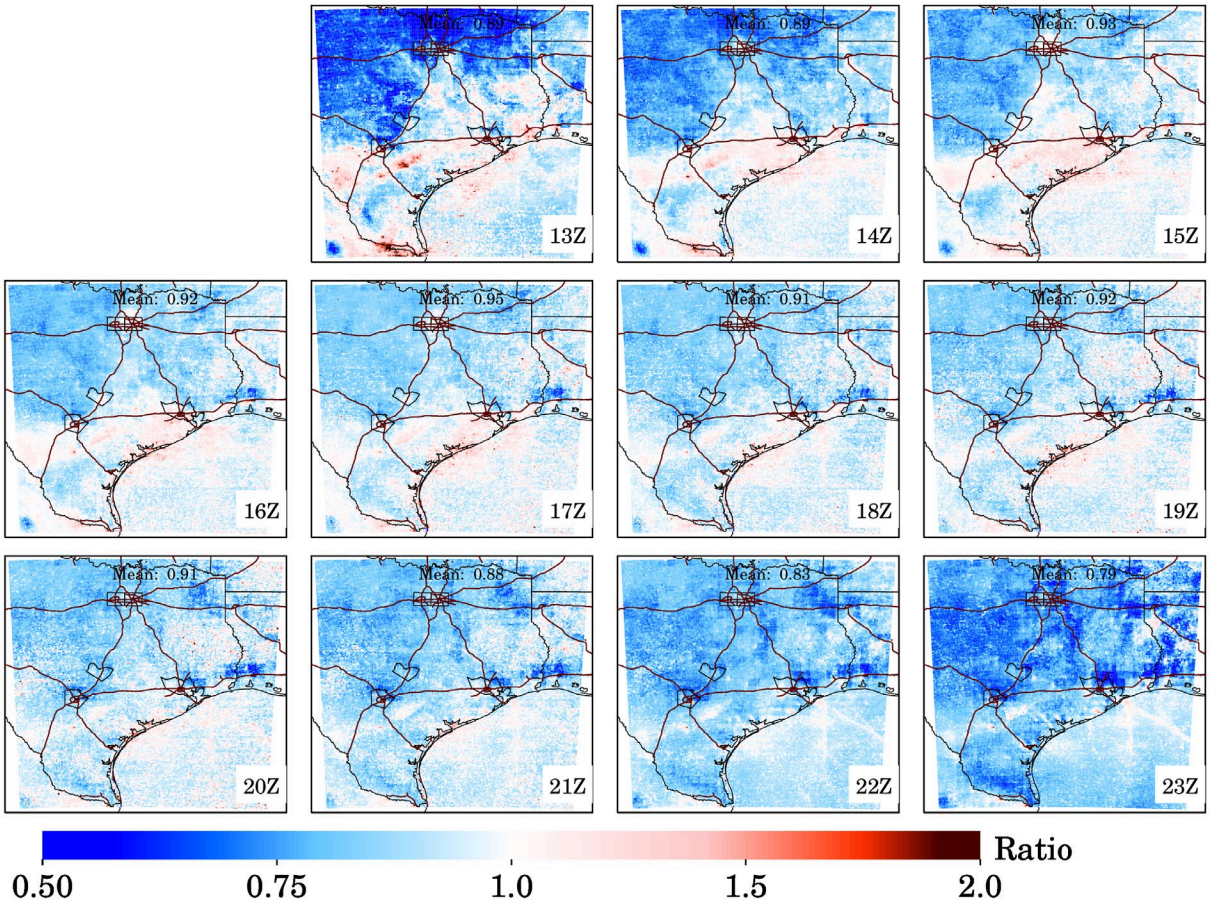

Figure 2.3.3. TEMPO NO_2 column amounts using CAMx AMF divided by TEMPO NO_2 VCD without CAMx AMF for all daylight hours. Each panel represents an individual hour (13Z – 23Z or 8 AM – 6 PM local time).

Focusing on Houston (Figure 2.3.4), one can more clearly see the NO_2 enhancements in the polluted sections of Houston now that spatial gradients due to ship channel emissions are able to be resolved, urban emissions and suburban emissions in CAMx (4 km) as opposed to GEOS-CF (~25 km).

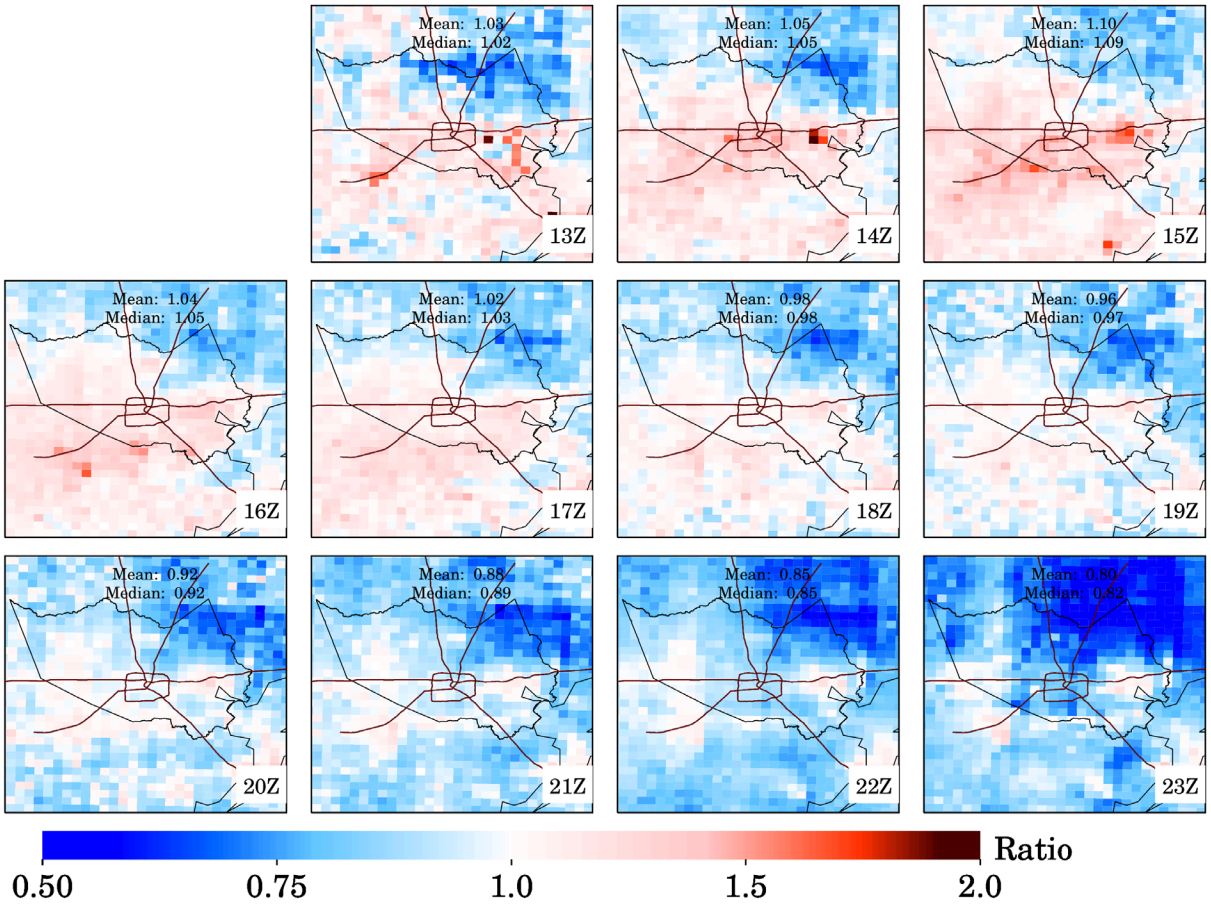

Figure 2.3.4. TEMPO NO_2 column amounts using CAMx AMF divided by TEMPO NO_2 column amounts without CAMx AMF for all daylight hours for the Houston metropolitan area. Each panel represents an individual hour (13Z – 23Z or 8 AM – 6 PM local time).

Next, the 37-day averaged CAMx column NO_2 VCD are compared with TEMPO column NO_2 VCD (see Figure 2.3.5). the focus of this analysis is on eight subregions (panels in figure) within the east Texas CAMx model domain: Austin, Dallas, Houston, San Antonio, an area in Northeast Texas (NE_TX), an area in West Texas (W_TX), an area in Deep East Texas (DeepE_TX) and a rural area between Houston and San Antonio (SE_TX); their spatial extents are shown in Figure 2.2.3. As discussed in Sections 2.1 and 2.4, the team conducted two CAMx simulations: Baseline (red) and Final (orange; shown as "Updated CAMx").

Figure 2.3.5 shows that the column NO_2 amounts from the Baseline CAMx simulation are larger than TEMPO column NO_2 for nearly every hour of every location. This strongly suggests an overestimate of NOx emissions and these results drove us to re-evaluate the biogenic NOx emissions. As described in Section 2.4, a new simulation with an updated soil NOx (NO and HONO) parameterization was implemented that substantially reduced soil NOx emissions. When comparing TEMPO column NO_2 to the updated CAMx column NO_2, there is better agreement in nearly all areas and timeframes, and especially in the rural areas most impacted by soil NOx emissions.

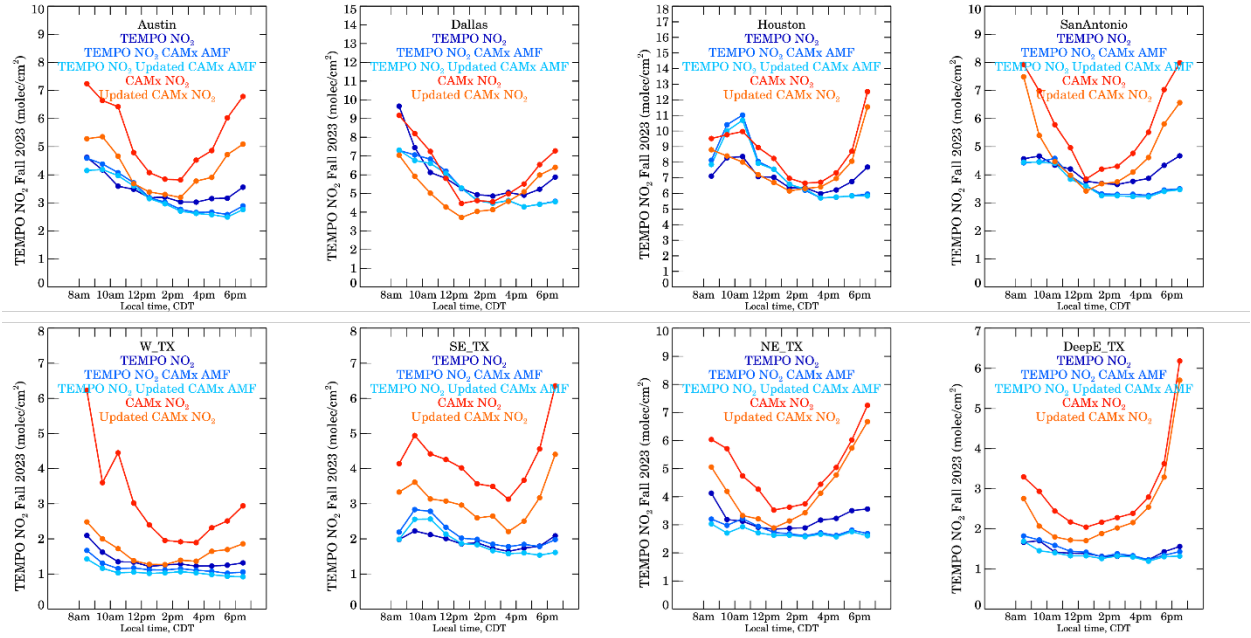

Figure 2.3.5. NO_2 column amounts for CAMx (red), Final CAMx (shown as "Updated CAMx"; orange), and three TEMPO NO_2 products (shades of blue) for the eight regions of interest. All TEMPO and CAMx NO_2 column amounts are averaged for the 37-day period between August 25, 2023 and September 30, 2023.

Discrepancies between the Updated CAMx column NO_2 and TEMPO column NO_2 become clearer when those two values are shown individually in Figure 2.3.6 and Figure 2.3.7. Over much of the area during most hours, CAMx column NO_2 remains larger than TEMPO NO_2 despite the reduction in soil NOx emissions. The magnitude of this bias varies by hour of day and location. In the early morning and late afternoon hours, the bias is larger (by ratio) than the bias in the mid-day timeframe. The bias is also largest over the Gulf suggesting that either there is a systematic error in TEMPO retrievals over water or that a marine-only NOx source (likely lightning NOx) is overestimated or some combination of both. The bias over land could be influenced by overestimates of both soil NOx and lightning NOx emissions.

Over urban areas with fractionally less biogenic emissions, there are different tendencies. During morning hours in Dallas and Houston, column NO_2 in CAMx is underestimated. This is also more clearly shown in Figure 2.3.8 and Figure 2.3.9. This suggests that urban NOx emissions are underestimated during these hours. Conversely, in the late afternoon there is a CAMx column NO_2 overestimate suggesting overestimated urban NOx emissions.

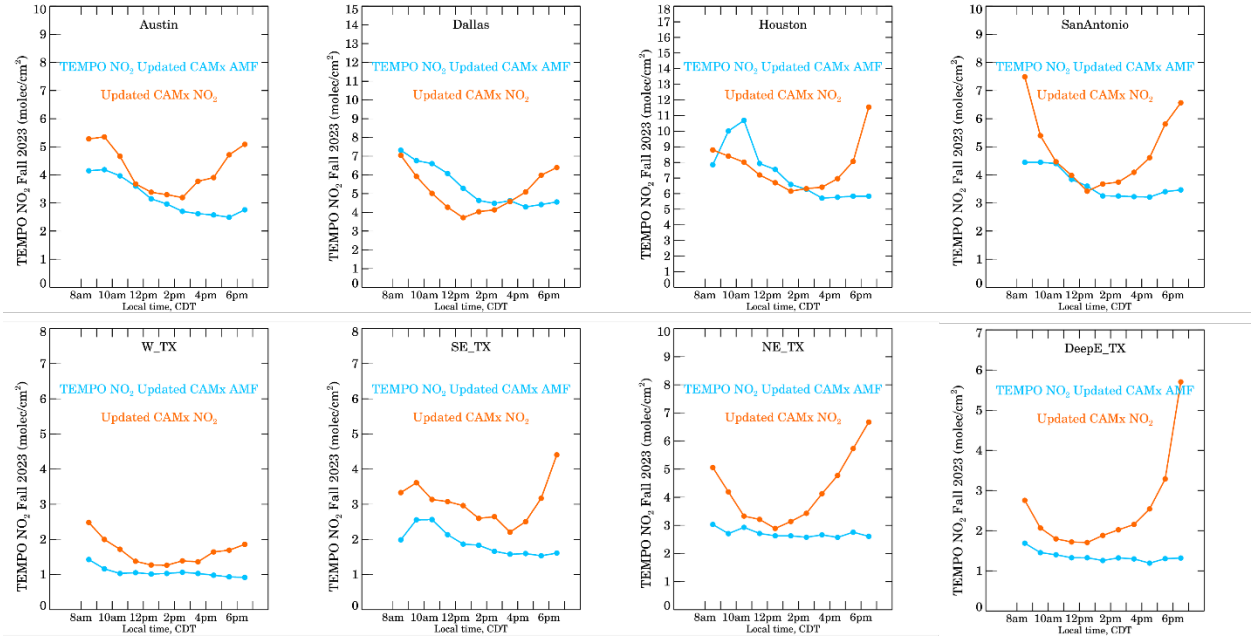

Figure 2.3.6. Final CAMx column NO_2 ("Updated" in figures; orange) and TEMPO (cyan) column NO_2 using Final CAMx AMF for the eight regions of interest. All TEMPO and CAMx NO_2 columns are averaged for the 37-day period between August 25, 2023 and September 30, 2023.

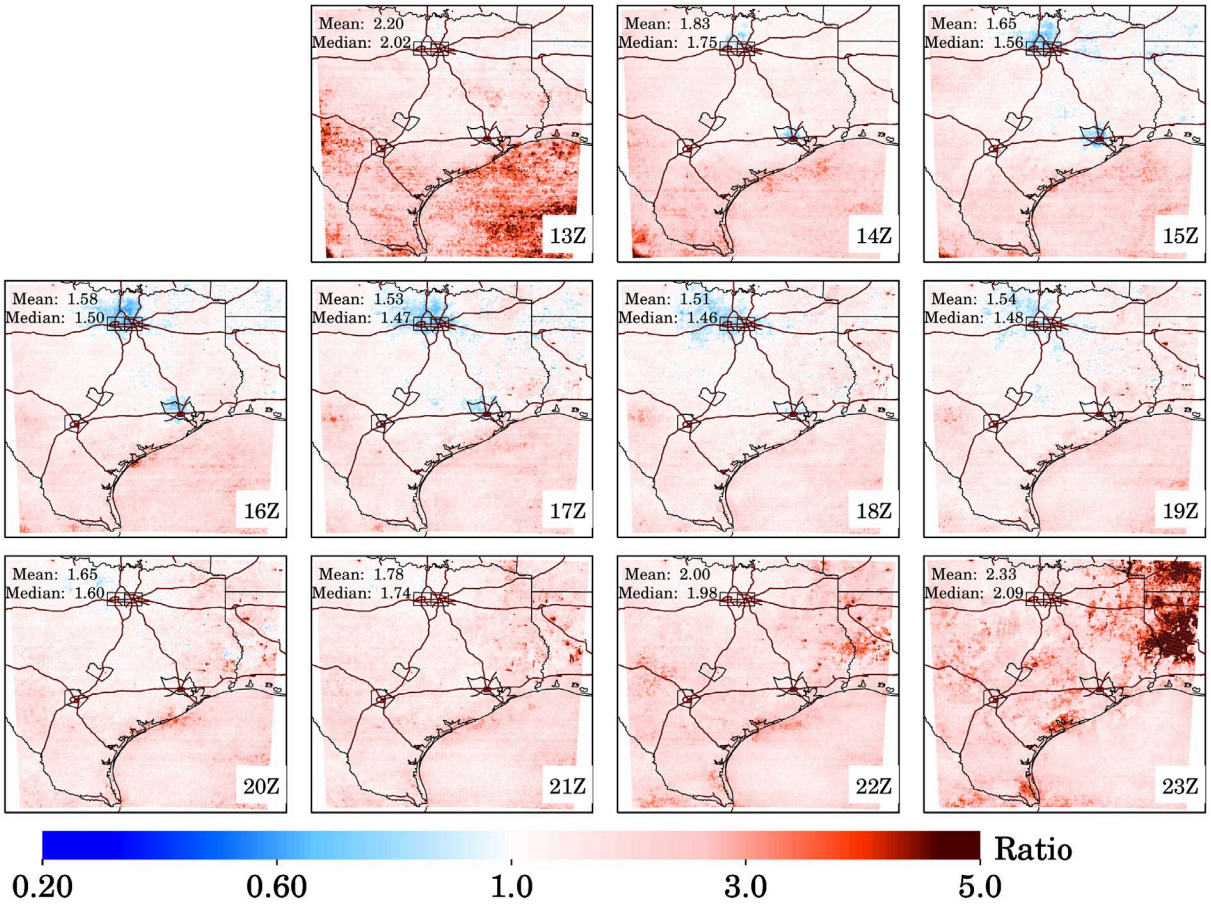

Figure 2.3.7. Ratio between Final CAMx NO_2 column amount and TEMPO NO_2 column amount using CAMx AMF averaged across the 37-day period between August 25, 2023 and September 30, 2023. Each panel represents an individual hour (13Z – 23Z or 8 AM –6 PM local time).

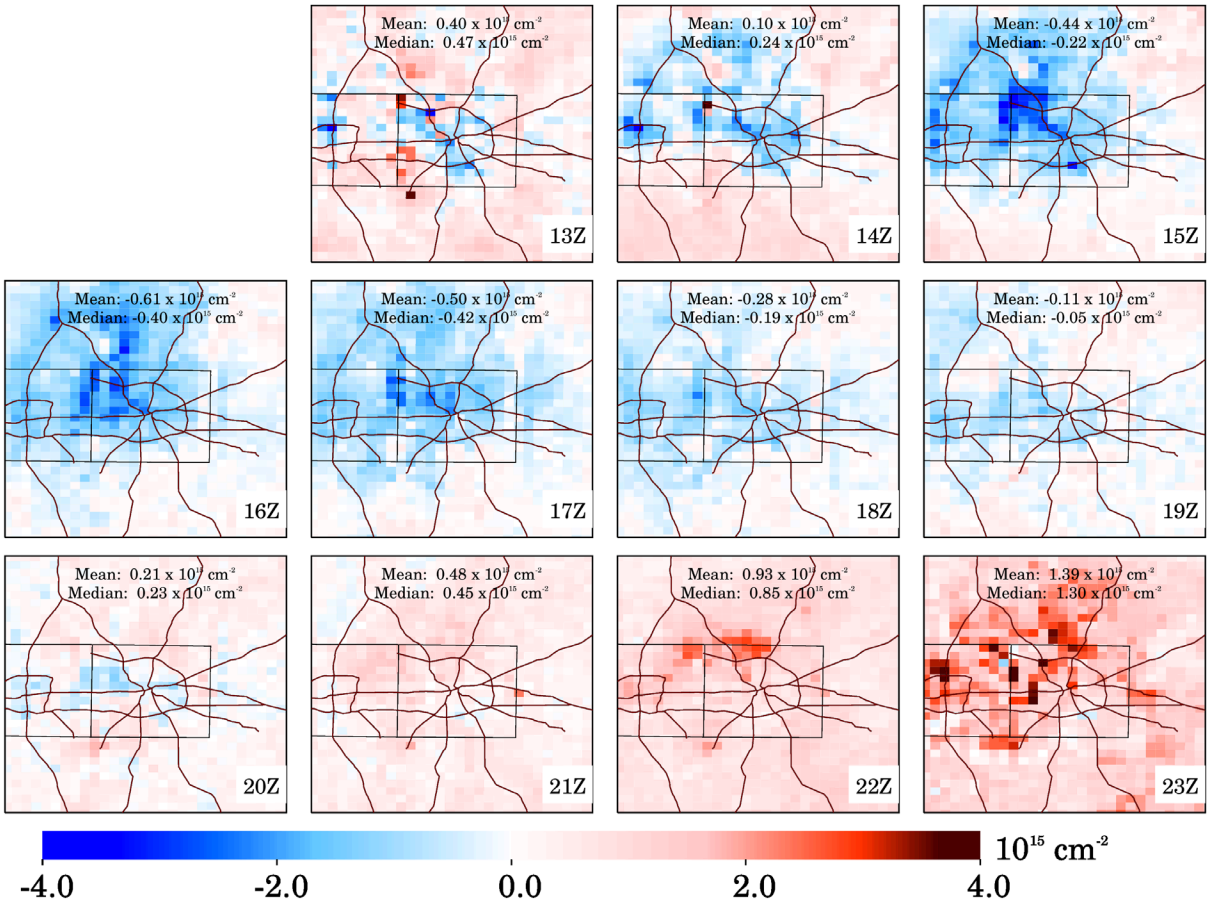

Figure 2.3.8. Ratio between Final CAMx column NO_2 column amount and TEMPO NO_2 column amount using Final CAMx AMF averaged across the 37-day period between August 25, 2023 and September 30, 2023, zoomed into the Dallas metropolitan area. Each panel represents an individual hour (13Z – 23Z or 8 AM – 6 PM local time).

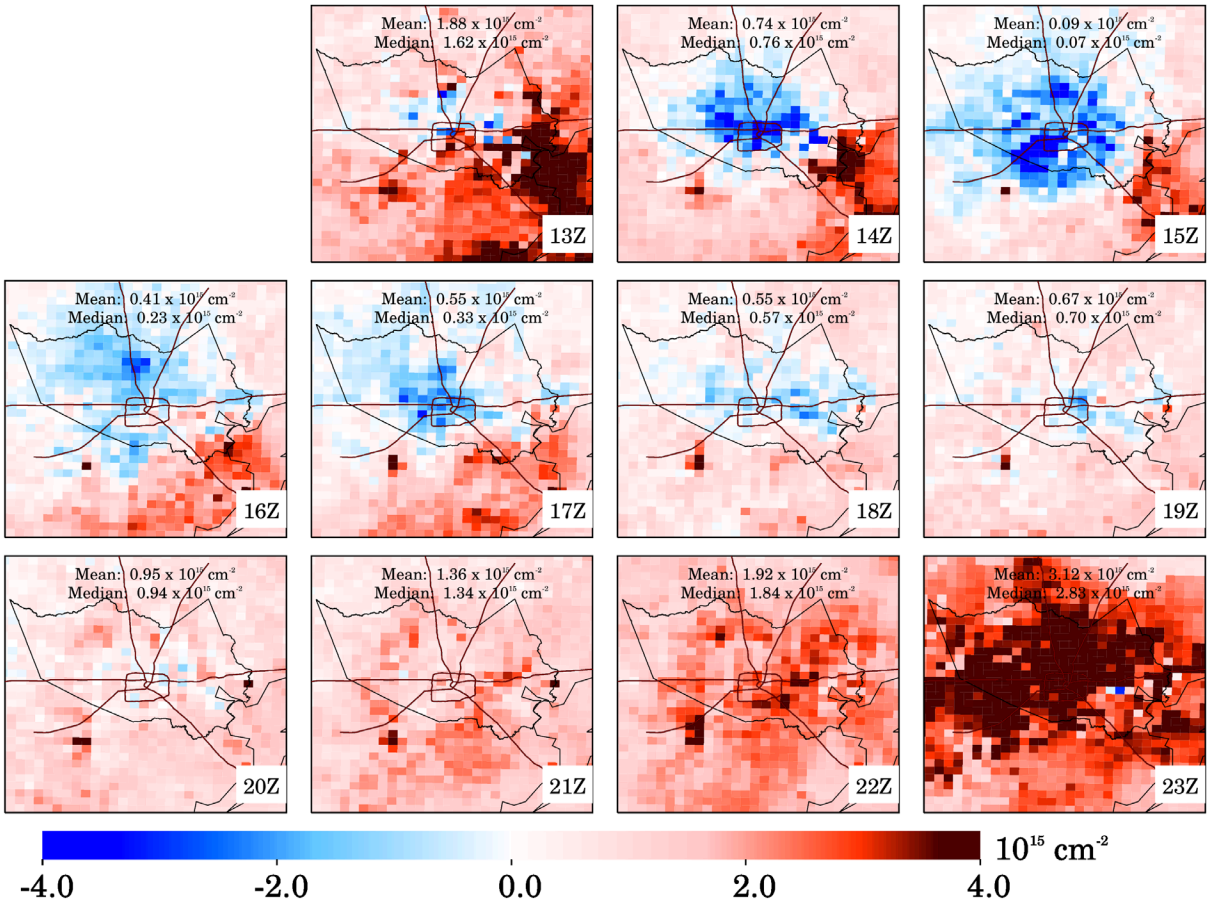

Figure 2.3.9. Ratio between CAMx column NO_2 VCD and TEMPO CAMx AMF NO_2 VCD averaged across the 37-day period between August 25, 2023 and September 30, 2023 now zoomed into the Houston metropolitan area. Each panel represents an individual hour (13Z – 23Z or 8 AM –6 PM local time).

The tagged CAMx simulation is helpful for quantifying the NO_2 impact of source sectors at any given location. In Dallas, vehicle NOx emissions (on-road and off-road) are the dominant sector impacting NO_2 (Figure 2.3.10) and thus, differences between CAMx and TEMPO in Dallas are likely attributed to these sectors. In Houston, the largest NOx underestimates occur between 14Z – 17Z (9 AM – 12 PM local time) and this time is also dominated by vehicle emissions. In rural areas, soil and lightning NOx are the dominant sectors impacting NO_2 (Figure 2.3.11) suggesting further revisions of these emission sectors. For further enhancements to the model, the following changes to the NOx emissions are suggested to bring the model simulation in better agreement with the TEMPO NO_2 measurements:

1. Investigation into the temporal allocation of on-road and off-road vehicle NOx emissions.
2. A further reduction of soil HONO and NO emissions. Further investigation into the decay period for available soil nitrogen from fertilizer, nitrogen deposition half-life, soil nitrogen availability for HONO, and fertilizer lifetime are suggested.
3. A reduction in lightning NOx emissions. Most recent published estimates of lightning NOx emissions suggest mol per flash rates are lower than previously thought: 100 – 200 mol per flash now as compared to past estimates which ranged from 200 – 500 mol per flash.

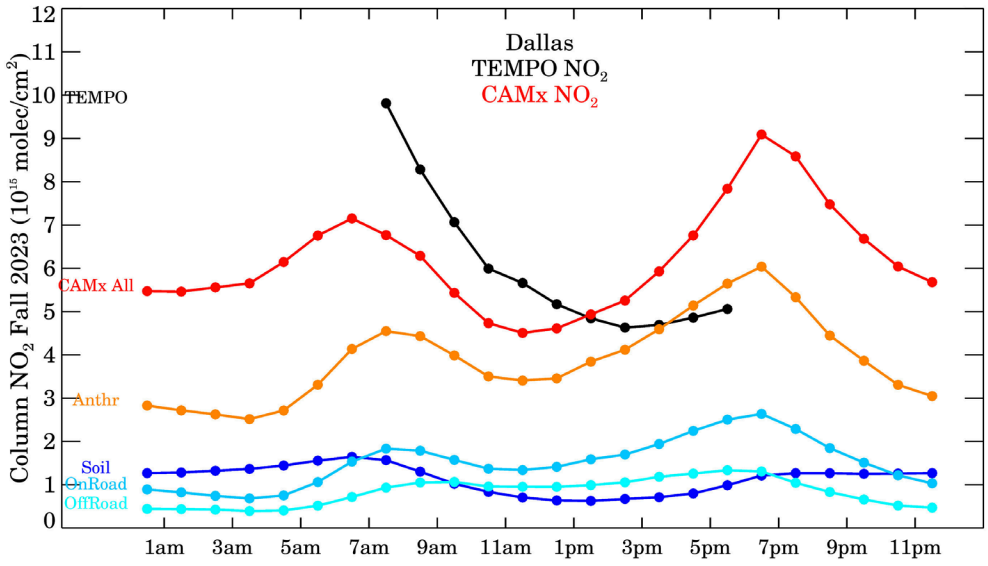

Figure 2.3.10. TEMPO NO_2 column (black) and tagged CAMx NO_2 columns (All: red; Anthropogenic: orange: Soil NOx: blue; On-road mobile: light blue; Off-road mobile: cyan) for Dallas.

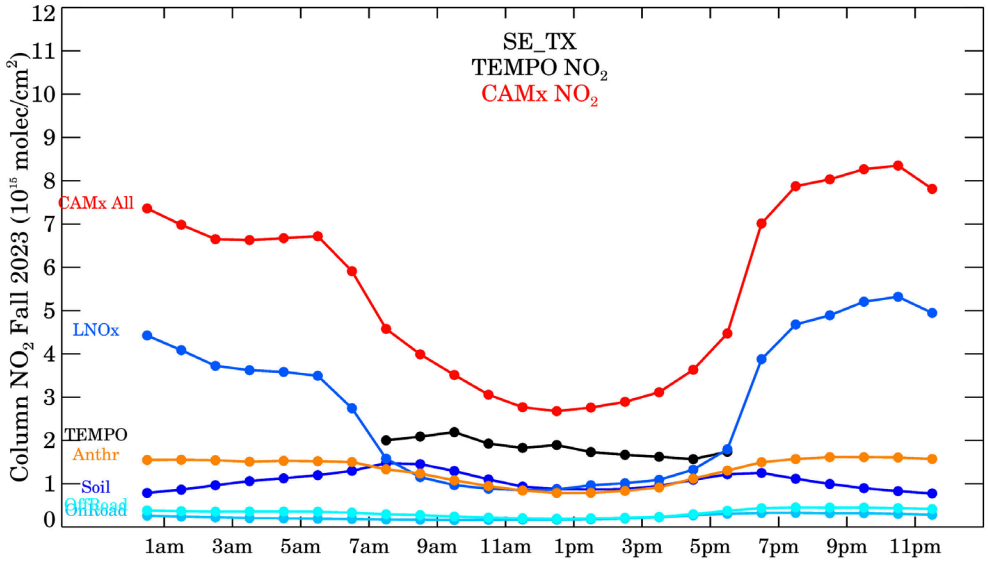

Figure 2.3.11. TEMPO NO_2 column (black) and tagged CAMx NO_2 columns (All: red; Lightning NOx: blue; Anthropogenic: orange: Soil NOx: blue; On-road mobile: light blue; Off-road mobile: cyan) for a rural area in Southeast Texas.

The tagged NO_2 in the simulation allows us to conduct a sensitivity study further reducing soil NO_2 and lightning NO_2 and when these are artificially halved, there is much better agreement with the TEMPO NO_2 measurements (Figure 2.3.12).

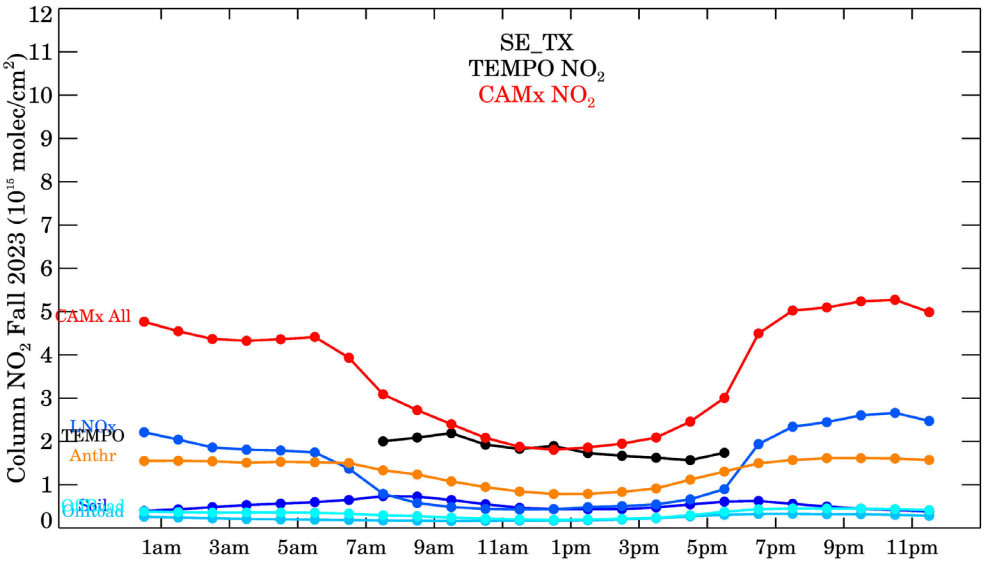

Figure 2.3.12. As in Figure 2.3.11, but with soil NO_2 and lightning NO_2 both halved.

2.4 Chemistry Updates and Testing

Following the Baseline CAMx simulation and subsequent model performance evaluation and comparison to TEMPO NO_2 columns, Ramboll performed a series of short CAMx sensitivity tests both with and without source apportionment to investigate changes to the MEGAN biogenic emissions, boundary conditions and a CAMx chemistry update involving organic nitrate (*p*NO3) photolysis. The team considered further CAMx updates involving vertical mixing, but the evaluation of surface NO_2 performance did not suggest that vertical mixing updates would lead to improved model performance.

The satellite comparison in Section 2.3 suggests that LNOx emissions in the Baseline simulation may be overestimated. Allen et al. (2021a) used TROPOMI, Geostationary Lightning Mapper (GLM) and the Earth Networks Total Lightning Network (ENTLN) to estimate LNOx production efficiency (PE; in units of NO mol per flash), and found estimates of around 150 mol per flash, which is lower than some previous estimates (Allen et al., 2010; 2021b; Ott et al., 2010). The CAMx LNOx emissions processor uses convective available potential energy (CAPE) diagnosed from WRF, which is then used as a surrogate to estimate flash rate (Luo et al., 2017; Price and Rind, 1992). A constant PE is applied within the tropics (25°N to 25°S; 100 mol per flash). But outside the tropics, the processor estimates PE using an exponential parameterization from Pickering et al. (2017). Therefore, one cannot simply scale the PE by a constant factor, and the team lacked sufficient time and resources to consider an alternative means of adjusting LNOx emissions. Further investigation into this issue is recommended.

Table 2.4.1 summarizes the configuration of the Baseline, sensitivity, and Final CAMx simulations. The sensitivity simulations are designed to explore the impacts of these changes to surface ozone and NO_2 as well as the comparison of column NO_2 to satellite measurements. The best performing options were then selected for the Final simulation to be conducted with 3-D outputs and source apportionment for the entire August 25 – September 30, 2023 modeling period. In this context, "best performing" relates to improvements in bias and error statistics across all CAMS and Dallas-Fort Worth, Houston and San

Antonio TCEQ regions. It also relates to improved agreement with the satellite measurements. The biogenic emissions updates to MEGAN v3.2.1 are described in Section 2.1.1.2.

Table 2.4.1. CAMx model configurations for Baseline, sensitivity, and Final simulations conducted as part of this project.

Run	Modeling Period	OSAT+3-D outputs	Biogenic Emissions	Boundary Conditions	Organic Nitrate Photolysis Update
Baseline	Aug 11 - Sep 30, 2023	Yes	MEGAN v3.21	2019 GEOS-Chem	No
Sens.run1	Aug 16 – Sep 2, 2023	No	MEGAN v3.21 with updates	2019 GEOS-Chem	No
Sens.run2	Aug 16 – Sep 2, 2023	No	MEGAN v3.2	2019 GEOS-Chem	No
Sens.run3	Aug 16 – Sep 2, 2023	No	MEGAN v3.2	2023 WACCM	No
Sens.run4	Aug 16 – Sep 2, 2023	Yes	MEGAN v3.21 with updates	2019 GEOS-Chem	No
Sens.run5	Aug 16 – Sep 2, 2023	Yes	MEGAN v3.21 with updates	2019 GEOS-Chem	Yes
Final	Aug 11 - Sep 30, 2023	Yes	MEGAN v3.21 with updates	2019 GEOS-Chem	Yes

2.4.1 Chemistry Updates

NOx concentrations in the free troposphere (FT) are sensitive to photochemical recycling from more oxidized nitrogen compounds (NOz) back to NOx (Murphy et al., 1993; Shah et al., 2023). The dominant FT NOz species by mass fraction are nitric acid (HNO_3), organic nitrates (ONs) and peroxyacetyl nitrate (PAN), and all the CAMx gas-phase chemical mechanisms include recycling of these NOz species to NOx via photolysis and/or reaction with HO radical. ONs and HNO_3 are likely to partition into the aerosol phase at the colder temperatures of the FT (Murphy et al., 1993) which could alter their photochemical fate. For example, enhanced photolysis of particle-phase nitrate ion (pNO_3) compared to gas-phase HNO_3 has been proposed as an important NOx-recycling mechanism in the marine boundary layer (MBL; Ye et al., 2016) although details are uncertain and poorly constrained by measurements (Gen et al., 2022). For ONs, Liu et al. (2012) found that particle-bound ONs can hydrolyze to pNO_3 and Zhao et al. (2023) found that these ON hydrolysis reactions occur for many ON compound structures. CAMx includes a simple parameterization of ON hydrolysis derived from Liu et al. (2012) and ambient measurements of Rollins et al. (2013). ONs that are hydrolyzed become unavailable for photolysis and/or OH-reactions that regenerate NOx.

The team considered updates to the CAMx treatments of NOx-recycling from HNO_3/pNO_3 and ONs. Implementing a scheme for enhanced pNO_3 photolysis was decided against because the overall importance remains uncertain and introducing a specific chemical interaction, e.g., dependence of pNO_3 photolysis on aerosol chloride content (Shah et al., 2023), is undesirable in the face of uncertainty. The CAMx treatment of ON hydrolysis was updated to consider aerosol phase-state, and therefore temperature/humidity, without introducing any dependence on aerosol composition.

2.4.1.1 Organic Nitrate Hydrolysis Update

Atmospheric aerosol particles can exist in various phase states, including liquid, semi-solid, and glassy solid (Shiraiwa et al., 2017). The main factors controlling aerosol phase state are chemical composition, relative humidity (RH), temperature (T) and particle size (Maclean et al., 2021). Molecular diffusivity is very sensitive to phase state and many orders of magnitude faster in liquid than glassy particles. The phase state of organic aerosol (OA) responds gradually to changing RH and T leading to gradual changes in viscosity whereas inorganic salts usually undergo sharp liquid-solid phase transitions. Mixtures of organic and inorganic species can also exhibit liquid-liquid phase separations (LLPSs) leading to particles that contain separate aqueous and organic solution phases. Aerosol phase state directly influences the occurrence and rate of chemical reactions including ON hydrolysis (Schmedding et al., 2020; Li et al., 2021).

The CAMx parametrization of ON hydrolysis (Hildebrandt Ruiz and Yarwood, 2013) was updated to consider reaction rate dependence on the molecular mixing time within aerosol particles. Maclean et al. (2021) parameterize Secondary Organic Aerosol (SOA) viscosity as a function of RH and T by combining detailed modeling with room-temperature viscosity data for simulated toluene SOA and toluene OA. Figure 2.4.1 (from Maclean et al, 2021) shows that the mixing time varies over 16 orders of magnitude from longer than 1 million hours for glassy particles (cold/dry conditions) to shorter than 1 billionth of an hour for liquid particles (warm/damp conditions) and they found similar behavior for pine tree SOA. Parametrized results from Maclean et al. were used to obtain equations for the percentage RH that produces a 6-minute mixing time (RH6m) for toluene SOA, pine tree SOA, and a mixture:

$$\text{RH6m (toluene SOA)} = -0.00513\ T^2 + 2.065\ T - 126.6$$
$$\text{RH6m (pine tree SOA)} = -0.007159\ T^2 + 2.899\ T - 183.2$$
$$\text{RH6m (mixed SOA)} = -0.005132\ T^2 + 2.065\ T - 126.6$$

The equation for mixed SOA was used to eliminate any dependence on SOA composition. Then, inorganic constituents were assumed to cause freezing point depression and lower the T for RH6m by 5K (Maclean et al., 2020) and that a transition between glassy solid and fully liquid states occurs over 20% RH range with relative reaction rate varying linearly between 0.05 for glassy solid aerosols to 1.0 for liquid aerosols. Figure 2.4.2 shows the resulting relative reaction rates for representative T & RH values that occur in the troposphere. The minimum value (0.05) occurs when a glassy solid aerosol state inhibits hydrolysis and the maximum value (1.0) occurs for liquid aerosols where the hydrolysis rate is unlimited by mixing. At 300 K, the updated parameterization is similar to the previous CAMx parameterization (which transitions between 20% and 40% RH) while generalizing the existing scheme to the full range of tropospheric conditions. In practice, the ON hydrolysis rate varies between 2.3×10^{-6} s^{-1} and 4.6×10^{-5} s^{-1} (ON lifetime of 120 hours to 6 hours) which is slower or faster than the nominal ON photolysis rate of 2.3×10^{-5} s^{-1}. Thus, aerosol phase state can modulate the dominant ON fate in CAMx between hydrolysis or photolysis.

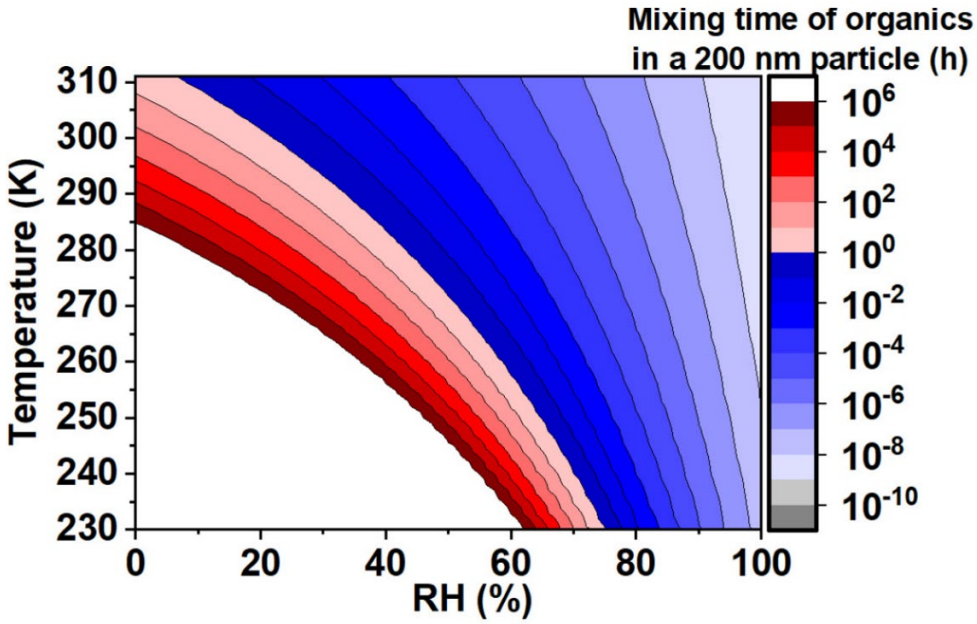

Figure 2.4.1. Dependence on T and RH of the mixing time of organic molecules within toluene SOA particles (from Maclean et al., 2021).

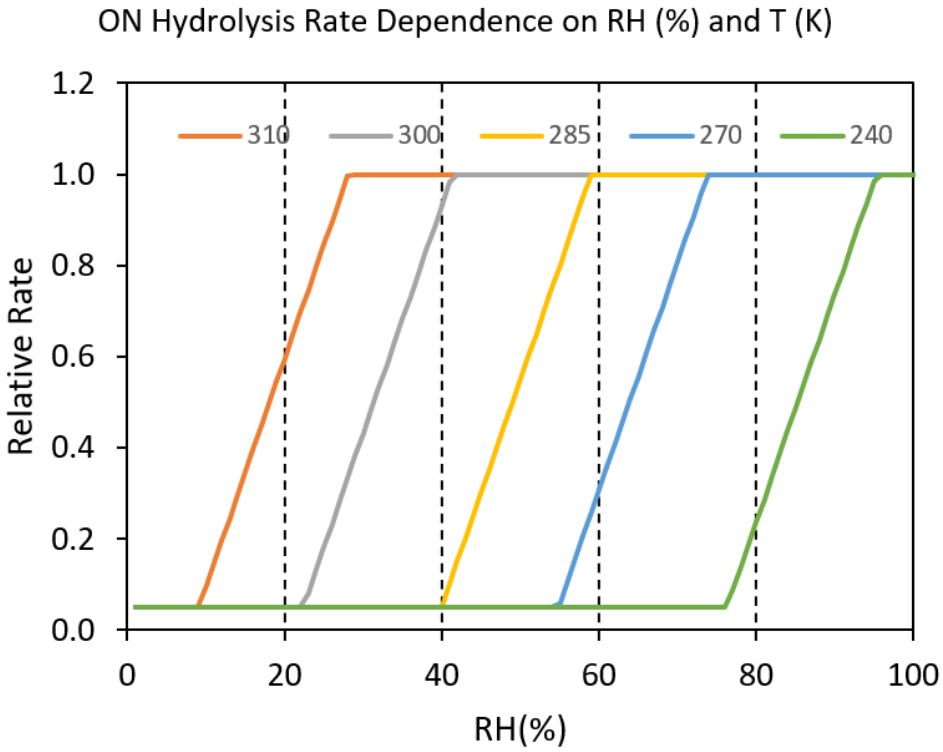

Figure 2.4.2. Relative ON hydrolysis rate (dimensionless) dependance on T (K) and RH (percent) for representative values that occur in the troposphere.

2.4.2 Comparison of Surface Model Performance Evaluation between Baseline and Final Simulation

Figure 2.4.3 shows maps of Baseline (top) and Final (bottom) CAMx mean bias across the entire modeling episode at each TCEQ CAMS NO_2 monitor. The MEGAN soil NOx emission reductions in the Final run reduce positive NO_2 biases in rural areas relative to the Baseline run. The substantial negative NO_2 biases in urban areas are made slightly larger by the soil NOx emission reductions. The positive NO_2 biases in oil and gas producing regions in the Baseline run are reduced slightly in the Final run (Karnes County C1070 mean bias reduced from +7.2 to +6.7 ppb).

During 2023, the high-sensitivity NOx instrument described in Section 2.1.2 collected NO_2 measurements adjacent to TCEQ's NOx instrument at Tyler Airport (CAMS 82) in Northeast Texas. To better understand the impact of the MEGAN soil NOx emission adjustments, the Baseline and Final modeled NO_2 concentrations were compared against these "true NO_2" measurements. The scatter plot in Figure 2.4.4 shows hourly (7 AM-5 PM CST to correspond with TEMPO availability) true NO_2 measurements and model pollutant concentrations (left panel: Baseline; right panel: Final) at the Tyler Airport. This is a rural location, as evidenced by the range of measured NO_2 concentrations. The MEGAN soil NOx emission adjustments in the Final CAMx run improve the NO_2 mean bias considerably (Baseline: +0.6 ppb; Final: -0.1 ppb), while also reducing the error (Baseline NME: 44.8%; Final NME: 38.2%).

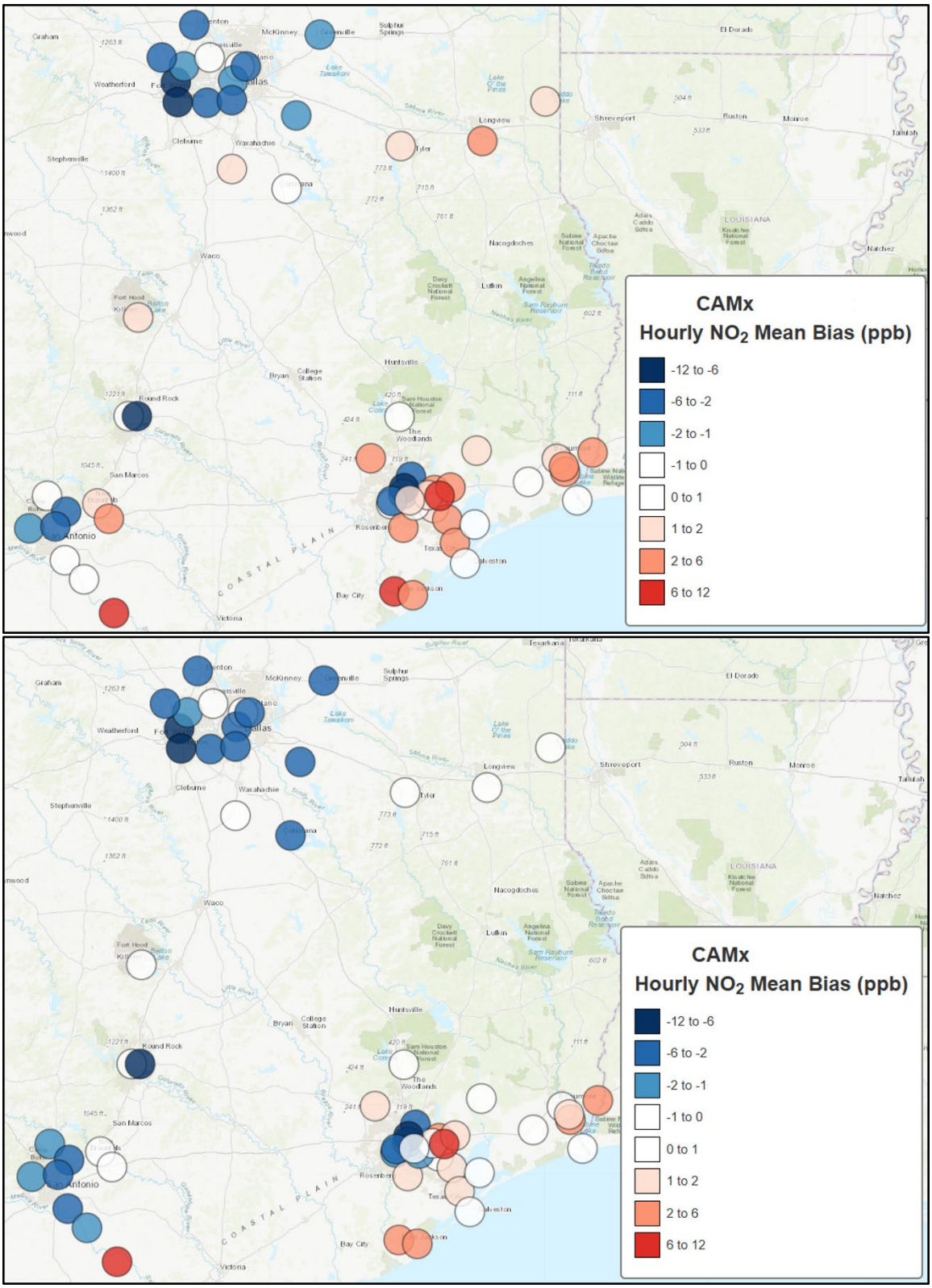

Figure 2.4.3. 7 AM-5 PM CST Baseline (top) and Final (bottom) CAMx NO_2 mean bias (ppb) at each TCEQ CAMS site averaged over the August 25-September 30, 2023 modeling period.

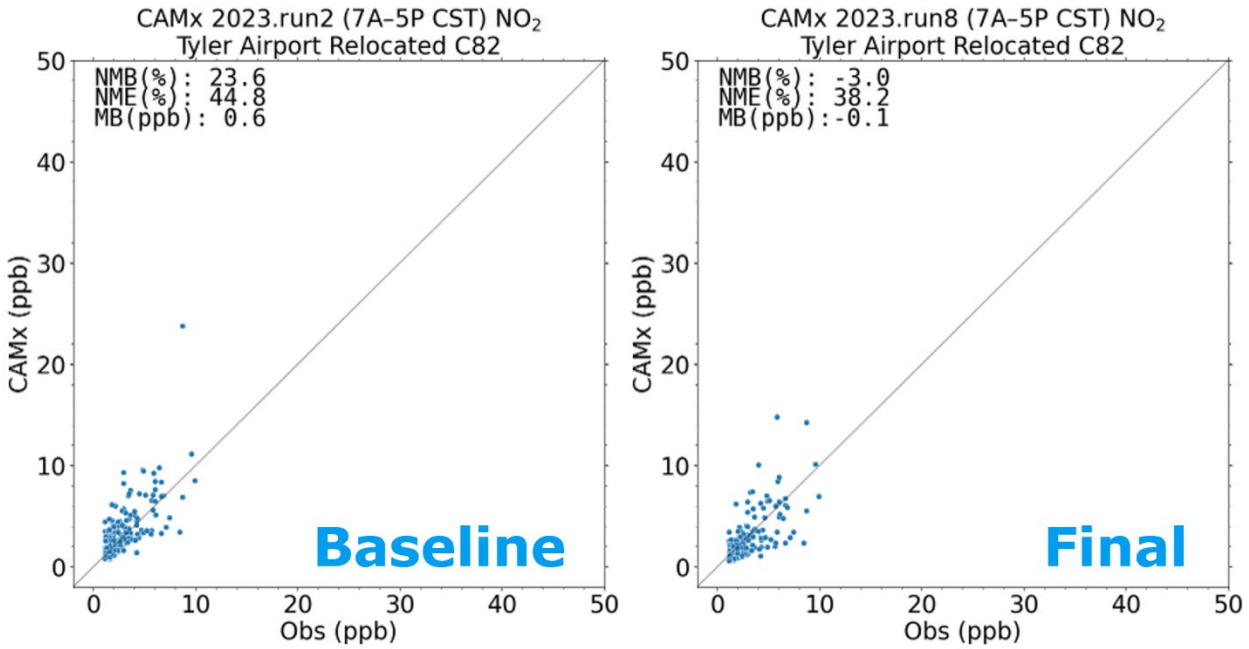

Figure 2.4.4. Hourly CAMx (7 AM-5 PM CST) NO_2 (left panel: Baseline; right panel: Final) plotted against observed NO_2 at Tyler Airport using high NOx sensitivity instrument during the August 25-September 30, 2023 modeling period.

Figure 2.4.5 shows scatter plots for CAMx MDA8 ozone compared to ozone observations at all CAMS in the CAMx 4-km domain (top row), Houston (bottom row) for the Baseline (left column) and Final (right column) runs. Figure 2.4.6 shows similar scatter plots for Dallas-Fort Worth (top row) and San Antonio (bottom row). The MEGAN soil NOx emission reduction in the Final run reduces the large positive ozone bias in the Baseline run substantially. Houston, Dallas-Fort Worth and Texas all have bias and error statistics that are within or close to the Emery et al. (2017) goal benchmarks (NMB: <±5%; NME: <15%) in the Final run. San Antonio also shows a substantial reduction in ozone bias in the Final run, but performance is worse (mean bias: +5.7 ppb) than the other regions (still within Emery et al. [2017] criteria benchmarks; NMB: <±15%; NME: <25%).

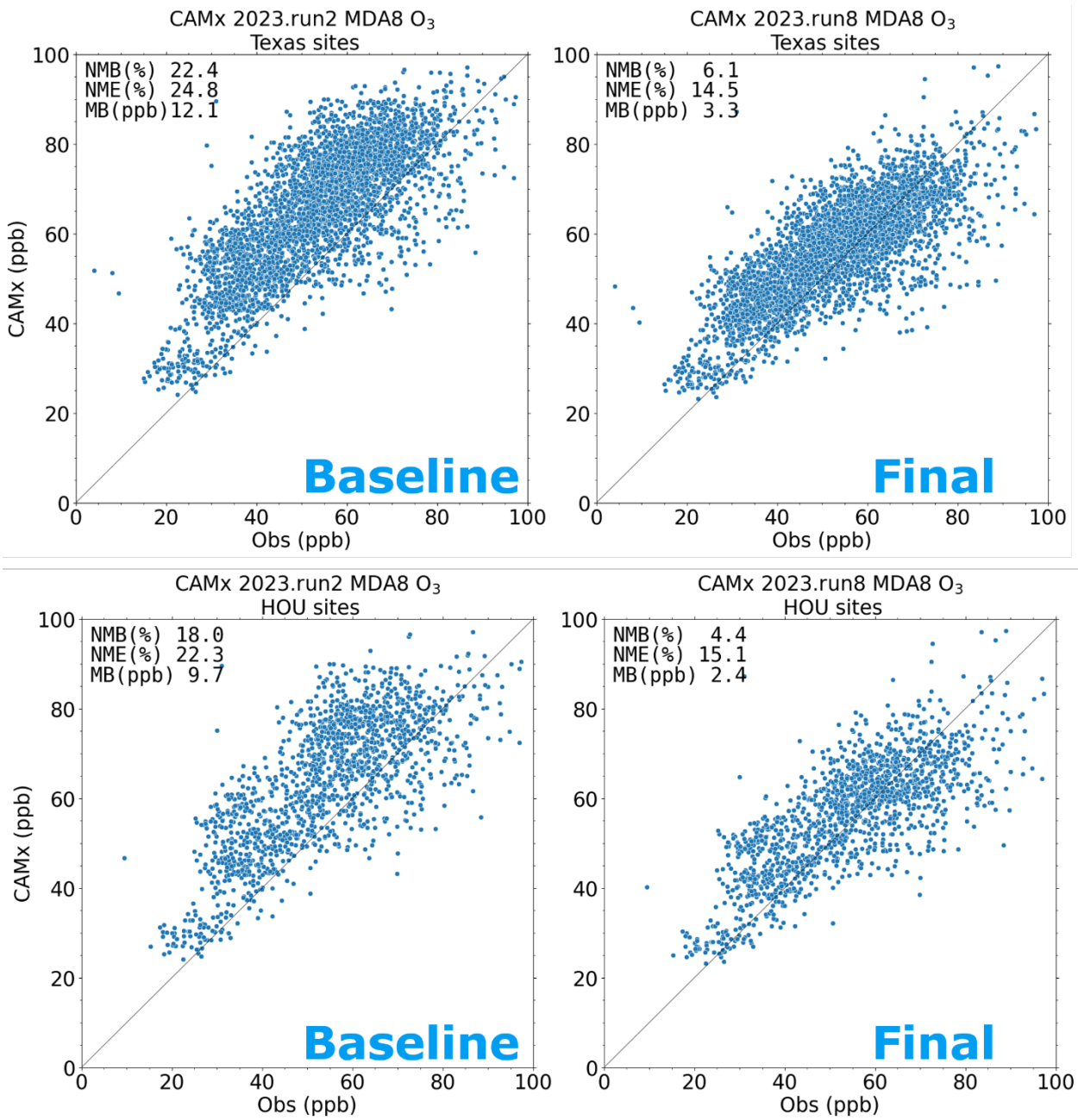

Figure 2.4.5. CAMx and observed MDA8 ozone across all TCEQ CAMS sites within Texas (top row) and Houston (bottom row) for the Baseline (left panels) and Final (right panels) simulations during the August 25-September 30, 2023 modeling period.

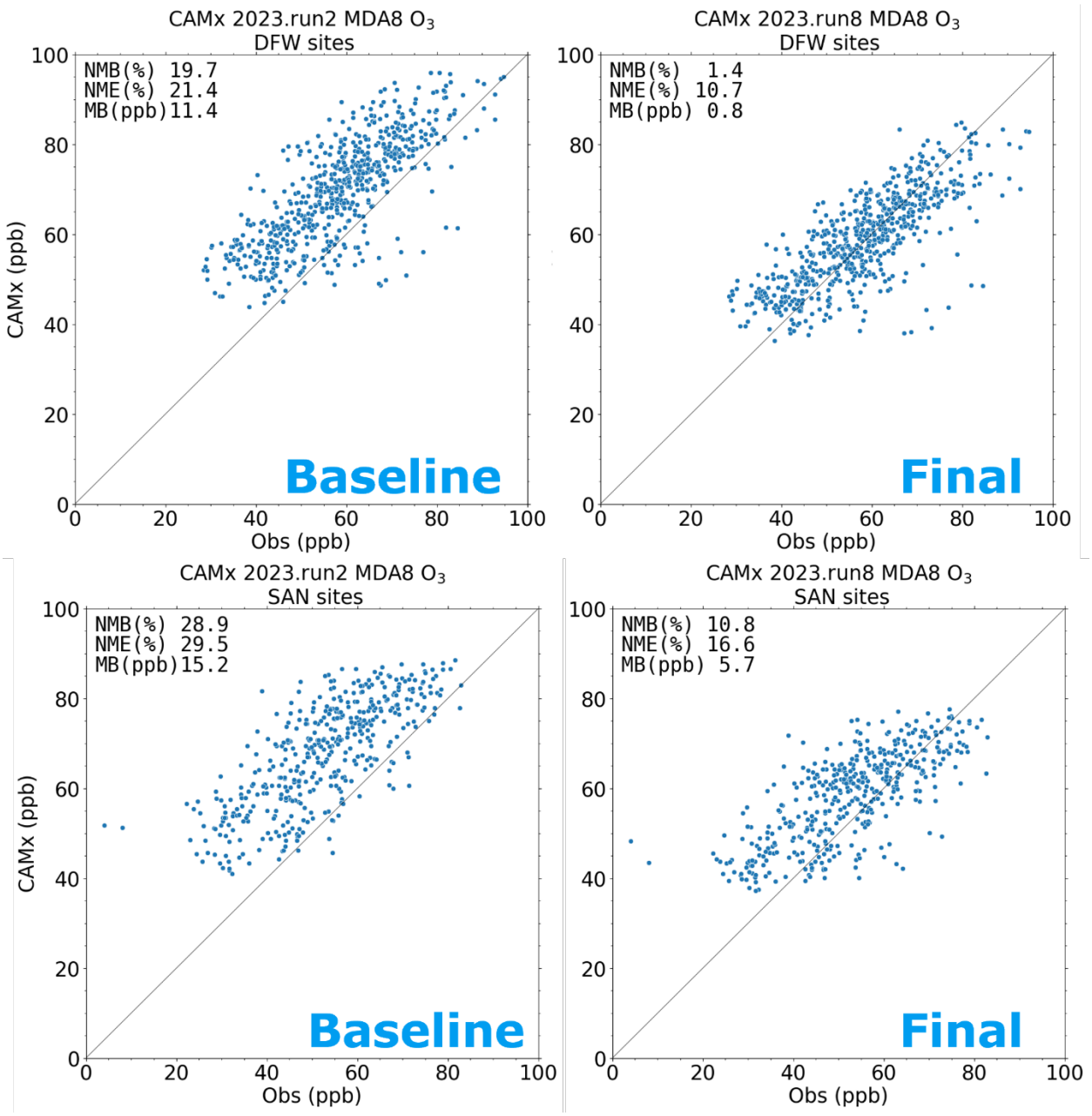

Figure 2.4.6. CAMx and observed MDA8 ozone across all TCEQ CAMS sites within Dallas-Fort Worth (top row) and San Antonio (bottom row) for the Baseline (left panels) and Final (right panels) simulations during the August 25-September 30, 2023 modeling period.

2.5 Estimating NOx Emissions by Sector and by Time of Day using CAMx Source Apportionment and TEMPO Retrievals

The flux divergence method can provide high resolution maps of NOx emissions using spatial remote sensing data. The method has been used to identify point sources and intra-urban variations using TROPOMI retrievals over Houston (Goldberg et al., 2022), cities in South Asia (de Foy and Schauer, 2022) and elsewhere around the world (Beirle et al., 2023). This method was applied to GCAS retrievals over Houston in AQRP 22-023 and it was able to identify major highways, shipping lanes in Galveston Bay and large point sources in the greater Houston area.

Flux divergence analysis was applied to TEMPO NO_2 retrievals over Texas, the first application of this method to TEMPO data, to the researchers' knowledge. Data from the full data record available was used, from August 2, 2023 to March 31, 2025. All hours available between 10 AM-4 PM CST were used. (It was found that the retrievals before and after those times were less reliable due to the increased solar zenith angle and therefore excluded them from the analysis.) Then individual swath pixels were screened using both the quality assurance flag, accepting only high-quality data, as well as using the effective cloud fraction, accepting pixels with values lower than 0.15. In total, between 2,000 and 3,500 retrievals were selected for each 4 km x 4 km grid cell in the analysis. Given the discussion above related to the visible signature of the GEOS-CF grid in the NO_2 VCD product, it was chosen to perform the flux divergence on the slant column density (SCD; rather than VCD), which does not suffer from these interferences.

Figure 2.5.1 shows the flux divergence results, which clearly identify the cities in Texas and large point sources. In addition, many of the highways show up as line sources using flux divergence, which is an improvement on prior results using TROPOMI retrievals (Goldberg et al., 2024; Sun, 2022). To obtain emission values from the flux divergence, a lifetime needs to be specified according to the equations shown in Beirle et al. (2019; 2021; 2023). Following their practice, a lifetime of 2 hours was used to obtain the emissions field in Figure 2.5.2. In effect, the emissions estimate is a combination of the flux divergence and the average NO_2 columns. The lifetime parameter determines the balance between the two, with a shorter lifetime giving more importance to the NO_2 columns. The shorter lifetime leads to a larger estimate of the emissions as it includes the effect of NO_2 destruction by photochemical reactions.

Similar NO_2 flux divergence maps are shown in Figure 2.5.3 over Central Texas (ranging from San Antonio to Waco; panel A). Dallas-Fort Worth (B), and Houston (C). These maps clearly show that the higher resolution of TEMPO and increased data availability relative to TROPOMI lead to improved detection of local features within individual urban areas. Airports stand out as significant areas of enhancement in the TEMPO signal. Large point sources are clearly visible. As mentioned above, the highways are also better characterized compared with previous analyses, including possibly detecting enhanced emissions at major intersections.

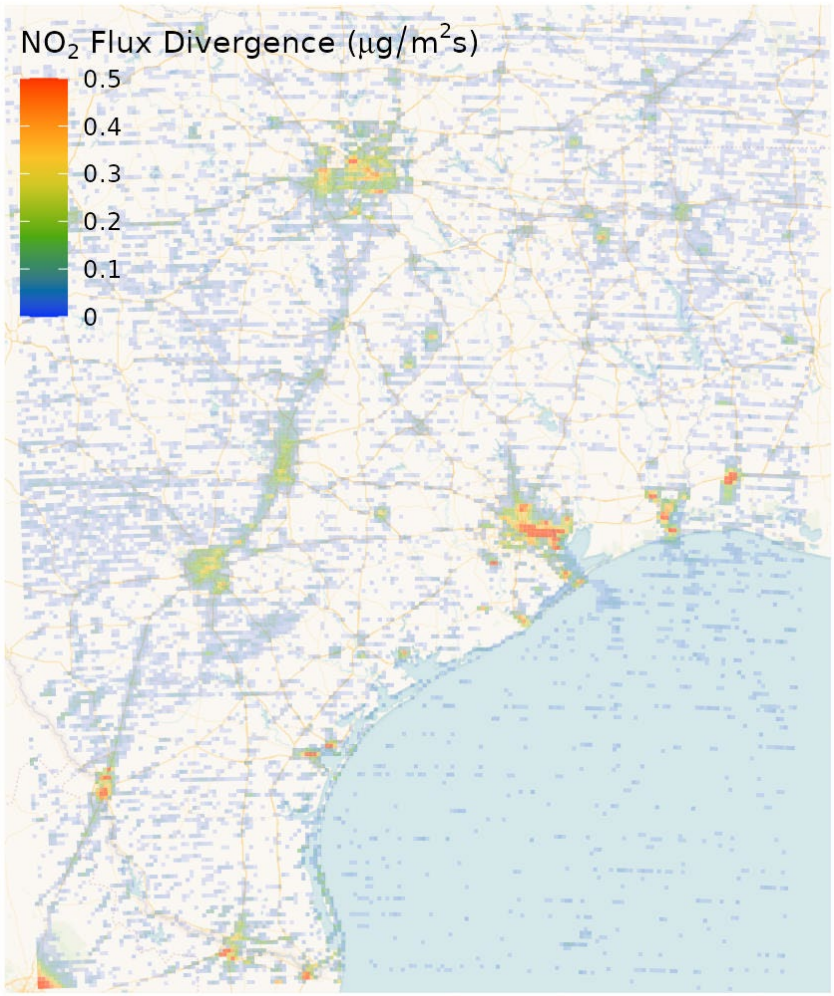

Figure 2.5.1. Flux divergence using all TEMPO data from Aug 2023 to Mar 2025 inclusive combined with 5th generation European Centre for Medium-Range Weather Forecasts atmospheric reanalysis (ERA5) 100-m surface winds on a 4-km grid.

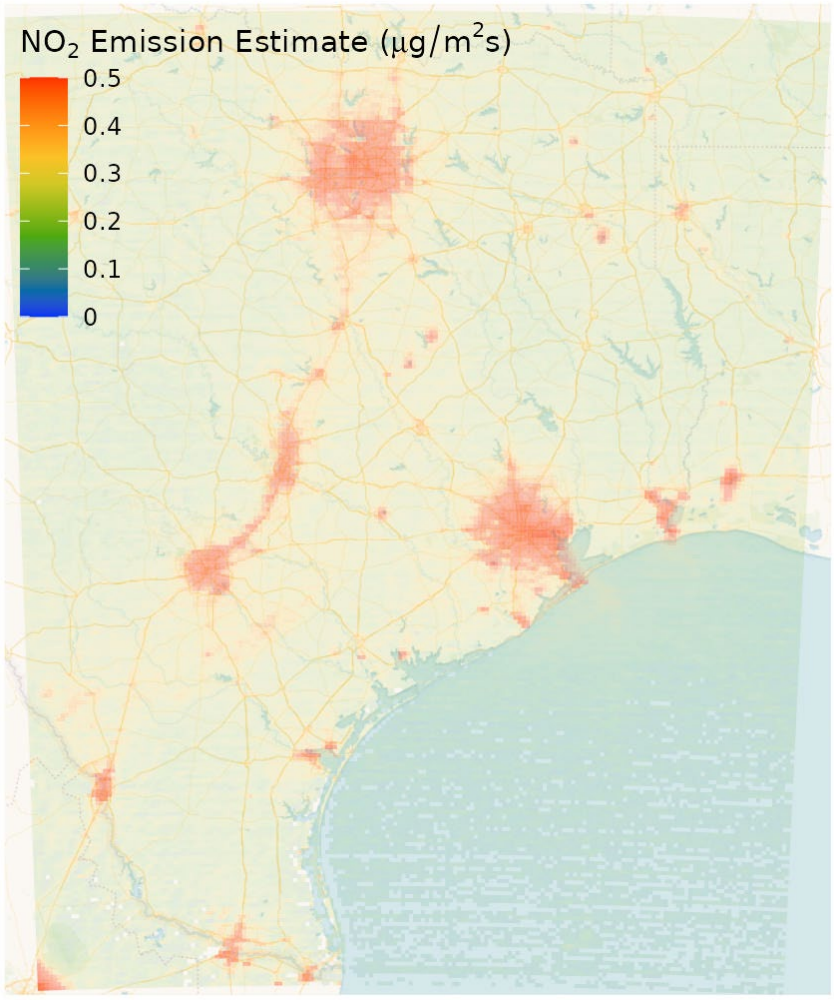

Figure 2.5.2. Emissions estimate based on flux divergence using all TEMPO data from August 2023 to March 2025, combined with ERA5 100-m surface winds on the CAMx 4-km grid.

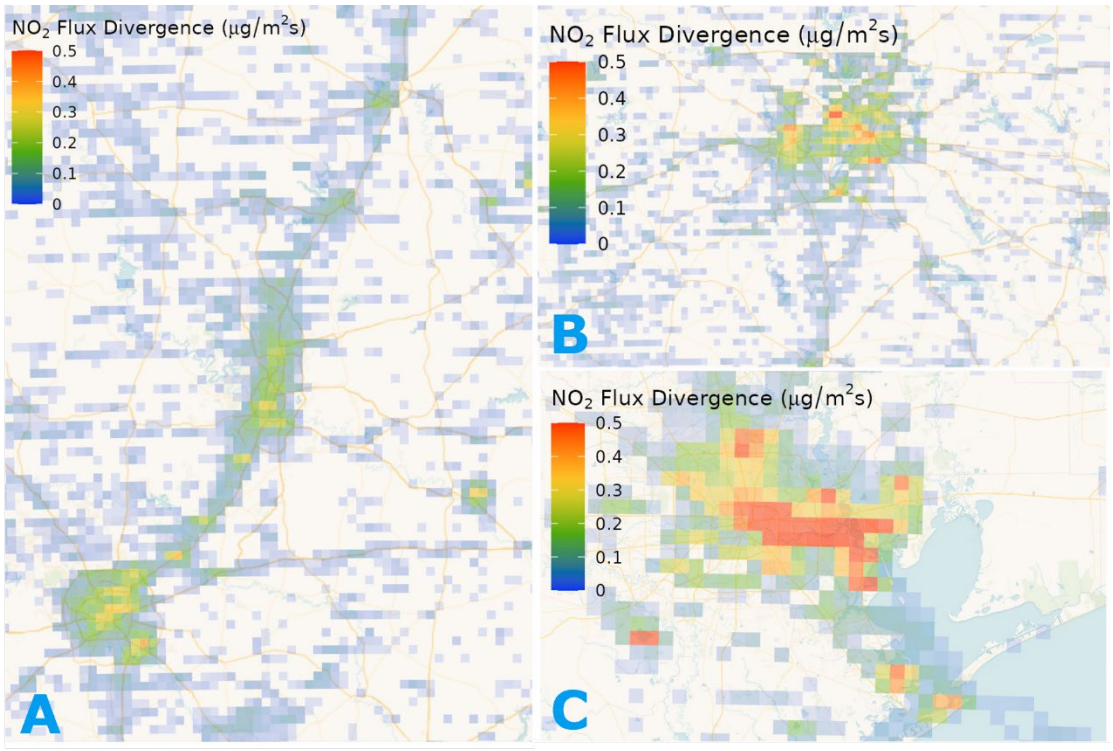

Figure 2.5.3. NO_2 flux divergence fields over (A) Central Texas, B) Dallas-Fort Worth, and C) Houston using all TEMPO data from August 2023 through March 2025.

As mentioned previously, the NO_2 SCD product was used to obtain a clear signal with the flux divergence method, using the complete data record available to date. Flux divergence fields were also generated by time of day (not shown). However, these hourly products display poor signal-to-noise ratio, and these products were not successful in obtaining diurnal profiles from these products. If it were possible to to extend the recalculation of the vertical columns with CAMx air mass factors for a year or more of TEMPO retrievals, this question could be revisited with improved results.

A Multiple Linear Regression (MLR) model was applied to identify the optimal combination of the individual emission sectors tagged in the Final CAMx simulation to match the TEMPO NO_2 vertical columns recalculated using the CAMx air mass factors. The MLR model follows the one developed for GCAS in AQRP 22-023. A bootstrap was performed on the individual scenes (date and time) included in the analysis followed by block-bootstrapping on the grid cells included from each scene. This provides an estimate of the uncertainty in the results. Further sensitivity tests were performed with different model configurations and found that the results presented here were robust relative to model specifications. The model was used to quantify modifications of each sector as a departure from the base case. An MLR factor of 0 corresponds to an optimal match, -1 to an elimination of that sector, 1 to a doubling of that sector. The values were constrained between –1 and 2. In addition to configuring MLR models for the entire domain, separate MLR model simulations for three subdomains were applied covering each of the Dallas-Fort Worth, Houston and Central Texas (includes San Antonio and Waco) regions. These subdomains are shown in Figure 2.5.3.

Figure 2.5.4 shows the Pearson correlation coefficient (r) for the Baseline CAMx NO_2 columns and the MLR-adjusted CAMx NO_2 columns relative to the TEMPO NO_2 VCD that uses CAMx air mass factors. This figure shows that the MLR model yielded significantly higher regression coefficients relative to the

Baseline CAMx simulation for the entire CAMx 4-km domain ("Texas" in figure labels) as well as for the three subdomains. The Texas correlation coefficient is considerably higher than any of Dallas-Fort Worth, Houston and Central Texas and has the smallest box of the four sampling grids.

Figure 2.5.5 shows the MLR coefficients for the entire Texas domain for 12:00 PM CST for the entire modeling period (August 25-September 30, 2023). The model suggests that on-road mobile emissions (positive factor in the figure) are underestimated and should be increased to improve the match with the TEMPO retrievals. Most other sectors need to be reduced according to the MLR model. In particular, the lightning sector does not match with the TEMPO retrievals and is eliminated by the MLR method.

The MLR simulations would greatly increase aircraft emissions. The figure shows a narrow box at a factor of 2, but the values would be larger than 2 and have larger uncertainty estimates if the constraint was removed. The team's understanding is that the current algorithm for TEMPO retrievals is affected by albedo issues, specifically with larger NO_2 signals over areas that are large and bright. This could be a confounding factor for airports (extensive areas with high albedos), which are better resolved in TEMPO than in TROPOMI retrievals (TEMPO native resolution is about twice that of TROPOMI).

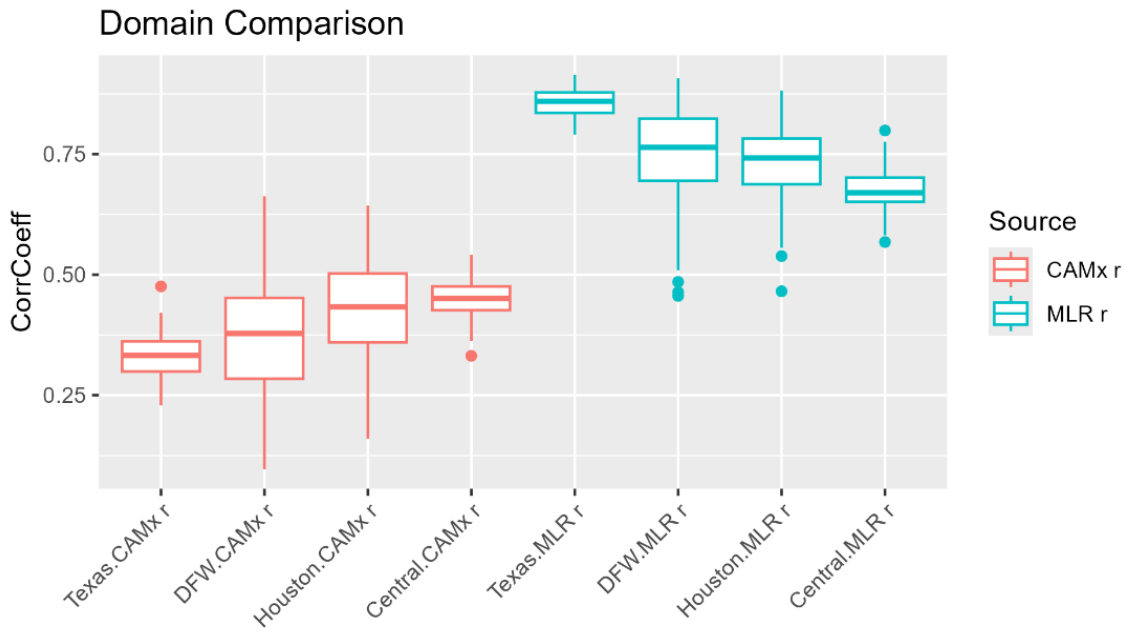

Figure 2.5.4. Pearson Correlation Coefficient (r) for the Final CAMx NO_2 columns and for the MLR adjusted CAMx NO_2 columns relative to the TEMPO NO_2 VCD using the CAMx air mass factors.

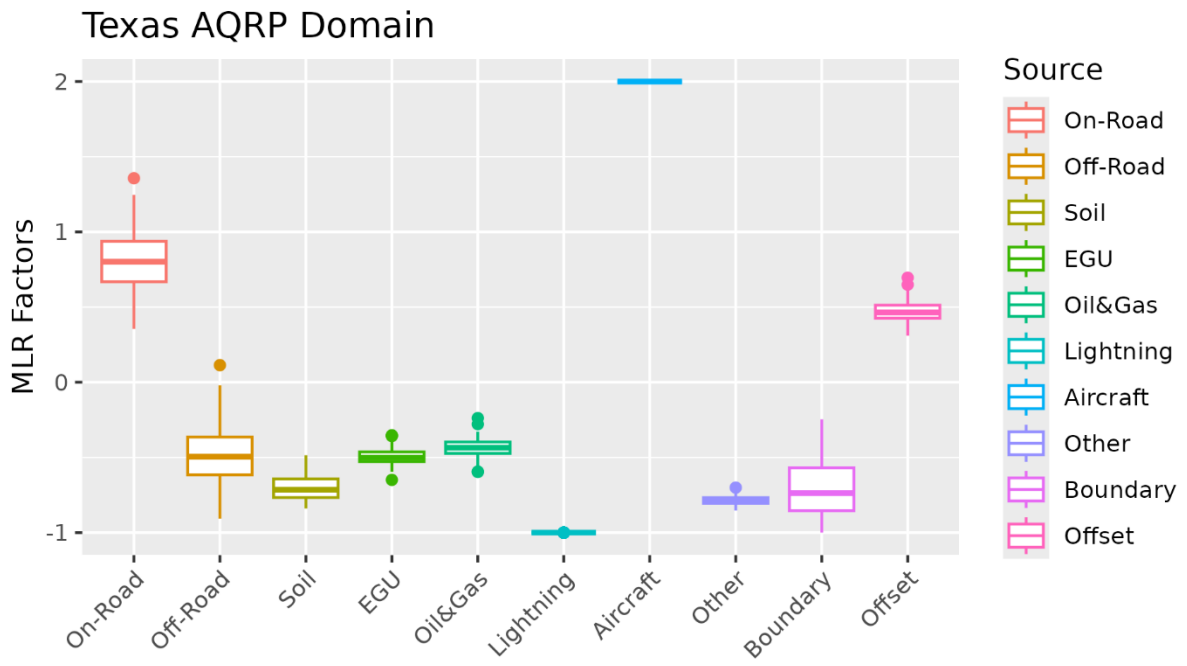

Figure 2.5.5. MLR adjustment factors for each sector in the analysis at 12:00 CST. 0 corresponds to optimal match, 1 to 100% increase, -1 to 100% decrease (i.e. "Zeroing out" the sector).

Figure 2.5.6 shows the same MLR adjustment factors as in the previous figure but extends to each subdomain (separate MLR models) in addition to the entire domain. There is broad consistency in the analysis across the subdomains with some notable differences. For example, the MLR models suggest that on-road mobile emissions should be increased for the whole domain and for Dallas-Fort Worth, but the factors are much closer to 0 for Houston and Central Texas. For off-road emissions, the models suggest decreases for the entire domain and for Houston but increases for Dallas-Fort Worth and Central Texas. MLR factors for the soil NOx sector suggest large reductions for all four regions. For Houston, the factors go down to –100%, whereas for Central Texas they are closer to –50%. The aircraft adjustment factor is at the maximum constraint for both Dallas-Fort Worth and Houston which have large airports but is highly uncertain (large box) for Central Texas where the airports are difficult for TEMPO to discern.

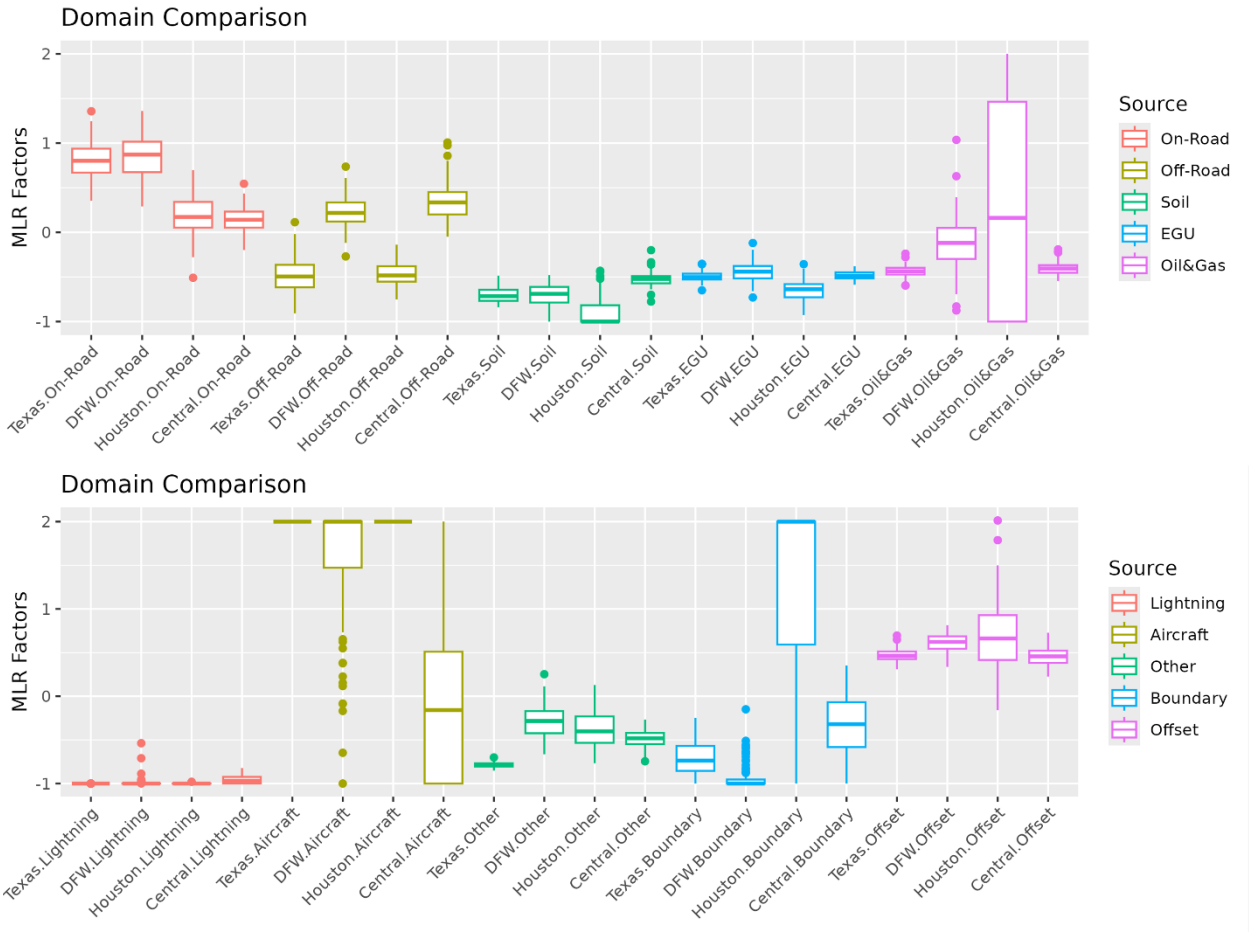

Figure 2.5.6. MLR adjustment factors by CAMx sector for the entire 4-km domain ("Texas" in figure labels) and for the three subdomains in the analysis: Dallas-Fort Worth ("DFW"), Houston ("Houston") and Central Texas ("Central").

3.0 CONCLUSIONS AND RECOMMENDATIONS FOR FUTURE WORK

The goal of this project was to understand whether NO_2 columns from the TEMPO satellite can constrain the NOx emissions in Houston and other Texas regions by source sector. This project is among the first to compare TEMPO NO_2 measurements with air quality model results.

3.1 Summary of Findings

In this project, the research team determined how TEMPO can be used for NOx emissions evaluation. TEMPO NO_2 measurements were used to evaluate CAMx model updates to NOx chemistry and the NOx emission inventory. Lessons learned and techniques developed for this project could be applied to other areas in the United States. The project also demonstrated the capability to estimate NOx emissions using the flux divergence method and multiple linear regression model applied to TEMPO NO_2 measurement.

While TEMPO provides hourly data resolution, the team found that the monthlong modeling period was not long enough to overcome the limitations imposed partially by the coarser spatial resolution. Other issues encountered with the TEMPO product (low sun angle measurements, high albedo, cloud obscured scenes, etc.) limited the comparison will likely improve over time.

The summary of findings separated by task is presented below:

Task 1:

- Aircraft climb-out (above 1 km) and cruise emissions were developed based on the EDGAR global database. Lightning NOx (LNOx) emissions were developed using Ramboll's LNOx processor.
- The BDSNP implementation in MEGAN was enhanced by implementing new temperature and soil moisture response functions, incorporating updated nitrogen deposition and fertilizer application data, and modeling HONO emissions. These updates have been integrated into the new version, MEGAN v3.21.
- CAMx Baseline model performance for MDA8 ozone showed a persistent positive bias (NMB: +22.4%; NME: 25.8%; mean bias: 12.1 ppb) across the CAMx 4-km domain.
- Performance against the NO_2 CAMS monitors showed better results than in AQRP 22-023. Across the CAMx 4-km domain, NMB was -27.8%, NME was 54.1% and the mean bias was -1.7 ppb.
- Examination of NO_2 performance at individual sites revealed consistent underpredictions at urban and near-roadway monitors and overpredictions at monitors in rural oil and gas producing regions

Task 2:

- In most areas, TEMPO NO_2 column amounts using GEOS-CF a priori information were largest in the morning hours (8 - 9 AM local time) decreasing until about 11 AM local time and flat throughout the rest of the day. The TEMPO NO_2 measurements were then re-processed with vertical NO_2 assumptions from CAMx and found discrepancies that underscore the enhanced uncertainties of TEMPO NO_2 in the mid-morning and late afternoon.
- NOx emission maps were then created from the TEMPO NO_2 measurements directly and found that NOx emissions are generally larger in CAMx than TEMPO, especially in a rural area southwest of Houston.
- It was found that TEMPO cannot capture the enhanced NOx from most point sources, although it can capture the largest point sources better than TROPOMI.

Task 3:

- CAMx generally had larger simulated column NO_2 amounts compared to TEMPO over most hours of the day and over most of the investigated subregions.
- CAMx NO_2 column overestimates were largest in the early morning, late afternoon, and over rural areas associated with soil and lightning NOx emissions.
- The large CAMx overestimates near daybreak and sunset could not be resolved, but this is suspected to be an issue with how the boundary layer is being resolved in the model during these hours. Future work should target these hours.
- It was also found that a CAMx NO_2 underestimate that was confined to urban areas during morning hours but changed to an overestimate in the late afternoon. Future work should investigate temporal allocation of anthropogenic emission sectors, including on-road and off-road mobile and industrial emissions.

Task 4:

- The CAMx parametrization of ON hydrolysis (Hildebrandt Ruiz and Yarwood, 2013) was updated to consider reaction rate dependence on the molecular mixing time within aerosol particles. This update showed near-zero impacts to surface NO_2 concentrations and only minor impacts in the free troposphere, which did not substantially change the NO_2 column amounts.
- The MEGAN soil NOx emission reductions in the Final run reduce positive NO_2 biases in rural areas relative to the Baseline run.
- The substantial negative NO_2 biases in urban areas are made slightly larger by the soil NOx emission reductions.
- The Baseline and Final modeled NO_2 concentrations was compared against "true NO_2" measurements in Northeast Texas and found that the MEGAN soil NOx emission adjustments in the Final CAMx run improve the NO_2 mean bias considerably (Baseline: +0.6 ppb; Final: -0.1 ppb), while also reducing the error (Baseline NME: 44.8%; Final NME: 38.2%).
- The MEGAN soil NOx emission reduction in the Final run reduces the large positive ozone bias in the Baseline run substantially. Houston, Dallas-Fort Worth and Texas all have bias and error statistics that are within or close to the Emery et al. (2017) goal benchmarks (NMB: <±5%; NME: <15%) in the Final run. San Antonio also shows a substantial reduction in ozone bias in the Final run, but performance is worse (mean bias: +5.7 ppb) than the other regions (still within criteria benchmarks).

Task 5:

- Flux divergence analysis was applied to TEMPO NO_2 retrievals over Texas—the first application of this method to TEMPO data, to the researchers' knowledge.
- This analysis clearly identifies the cities in Texas, large point sources and many of the highways (an improvement on prior results using TROPOMI retrievals), but needed the full TEMPO measurement record currently available (over 1.5 years) to reveal these features.
- It was also found that retrievals before 10 AM and after 4 PM CST were less reliable due to large solar zenith angle, but the quality of these retrievals could improve in future TEMPO product releases.
- Several (East Texas, Dallas-Fort Worth, Houston and Central Texas) multiple linear regression (MLR) models were applied together with CAMx tagged column NO_2 information and TEMPO NO_2 column measurements to evaluate NOx emission inventory sectors, following the MLR model developed for GCAS in AQRP 22-023.
- The MLR models suggest that on-road mobile emissions are underestimated in Dallas-Fort Worth and East Texas overall, but Houston and Central Texas on-road mobile emissions show much better agreement (smaller underestimates) with TEMPO columns.

- The MLR results suggest that most other sectors need to be reduced, including lightning and soil NOx. Further evaluation of these emission sectors using CAMx together with TEMPO column measurements is suggested.

3.2 Recommendations for Future Work

The following is recommended for future work:

- Investigate refinements to soil HONO and NO emissions, which could include further adjustments to soil temperature and moisture, decay period for available soil nitrogen from fertilizer, nitrogen deposition half-life, soil nitrogen availability for HONO, and fertilizer lifetime.
- Investigate refinements to lightning NOx, aircraft cruise and climb-out emissions.
- Investigate temporal allocation and overall magnitude of on-road and off-road vehicle NOx emissions, particularly in Dallas-Fort Worth.
- Repeat satellite comparison with tagged CAMx NO_2 columns as improved TEMPO retrievals are made available.
- Develop new CAMx modeling platform for one year or more to enable the use of CAMx air mass factors in the development of TEMPO NO_2 VCDs that remove the artifacts of the GEOS-CF a priori information.

4.0 AUDITS OF DATA QUALITY

Quality Assurance/Quality Control (QA/QC) procedures were performed in accordance with the Quality Assurance Project Plan (QAPP) completed at the beginning of this project. Per requirements for Category III projects, data audits on at least 10% of the data sets were peformed. In this section, the results of the QA/QC are reported.

4.1 WRF and CAMx simulations

The WRF and CAMx model simulations were run by Ramboll. Spatial maps of WRF and WRFCAMx near-surface meteorological variables were inspected for reasonableness. WRF temperature, humidity, wind speed and wind direction were compared with available airport observations during the modeling period. Ambient NO_2 concentrations simulated by the CAMx modeling were compared with all available ground-based observations of NO_2 and ozone during the modeling period, as detailed in Section 2.1 and 2.4.

4.2 TROPOMI screening

All TROPOMI data where the quality assurance flag was greater than 0.75 were used. This screened out pixels with optically thick clouds.

4.3 TEMPO screening

All TEMPO data where individual swath pixels passed the data quality check (main_data_quality_flag = 0) and effective cloud fraction was lower than 15% (eff_cloud_fraction < 0.15) were used.

5.0 REFERENCES

Allen, D., Pickering, K.E., Bucsela, E., Van Geffen, J., Lapierre, J., Koshak, W. and Eskes, H., 2021a. Observations of lightning NOx production from Tropospheric Monitoring Instrument case studies over the United States. *Journal of Geophysical Research: Atmospheres*, *126*(10), p.e2020JD034174.

Allen, D.J., Pickering, K.E., Lamsal, L., Mach, D.M., Quick, M.G., Lapierre, J., Janz, S., Koshak, W., Kowalewski, M. and Blakeslee, R., 2021b. Observations of lightning NOx production from GOES-R post launch test field campaign flights. Journal of Geophysical Research: Atmospheres, 126(8), p.e2020JD033769.

Beirle, S., Borger, C., Dörner, S., Li, A., Hu, Z., Liu, F., et al. (2019). Pinpointing nitrogen oxide emissions from space. *Science Advances*, *5*(11), eaax9800. https://doi.org/10.1126/sciadv.aax9800

Beirle, S., Borger, C., Dörner, S., Eskes, H. J., Kumar, V., De Laat, A., & Wagner, T. (2021). Catalog of NOx emissions from point sources as derived from the divergence of the NO_2 flux for TROPOMI. *Earth Syst. Sci. Data*, *13*, 2995–3012. https://doi.org/10.5194/essd-13-2995-2021

Beirle, S., Borger, C., Jost, A., & Wagner, T. (2023). Improved catalog of NOx point source emissions (version 2). *Earth System Science Data*, *15*(7), 3051–3073. https://doi.org/10.5194/essd-15-3051-2023

Canty, T.P., Hembeck, L., Vinciguerra, T.P., Anderson, D.C., Goldberg, D.L., Carpenter, S.F., Allen, D.J., Loughner, C.P., Salawitch, R.J. and Dickerson, R.R., 2015. Ozone and NO x chemistry in the eastern US: evaluation of CMAQ/CB05 with satellite (OMI) data. Atmospheric Chemistry and Physics, 15(19), pp.10965-10982.

Crippa, M., Guizzardi, D., Butler, T., Keating, T., Wu, R., Kaminski, J., Kuenen, J., Kurokawa, J., Chatani, S., Morikawa, T., Pouliot, G., Racine, J., Moran, M. D., Klimont, Z., Manseau, P. M., Mashayekhi, R., Henderson, B. H., Smith, S. J., Suchyta, H., Muntean, M., Solazzo, E., Banja, M., Schaaf, E., Pagani, F., Woo, J.-H., Kim, J., Monforti-Ferrario, F., Pisoni, E., Zhang, J., Niemi, D., Sassi, M., Ansari, T., and Foley, K.: The HTAP_v3 emission mosaic: merging regional and global monthly emissions (2000–2018) to support air quality modelling and policies, Earth Syst. Sci. Data, 15, 2667–2694, doi:10.5194/essd-15-2667-2023, 2023.

Curier, R.L., Kranenburg, R., Segers, A.J.S., Timmermans, R.M.A. and Schaap, M., 2014. Synergistic use of OMI NO_2 tropospheric columns and LOTOS–EUROS to evaluate the NOx emission trends across Europe. Remote Sensing of Environment, 149, pp.58-69.

de Foy, B., Lu, Z., Streets, D. G., Lamsal, L. N., & Duncan, B. N. (2015). Estimates of power plant NOx emissions and lifetimes from OMI NO_2 satellite retrievals. *Atmospheric Environment*, *116*(2), 1–11. https://doi.org/10.1016/j.atmosenv.2015.05.056

de Foy, B. (2018). City-level variations in NOx emissions derived from hourly monitoring data in Chicago. *Atmospheric environment*, *176*, 128-139.

de Foy, B., & Schauer, J. J. (2022). An improved understanding of NOx emissions in South Asian megacities using TROPOMI NO_2 retrievals. *Environmental Research Letters*, *17*(2), 024006. https://doi.org/10.1088/1748-9326/ac48b4

Emery, C., Liu, Z., Russell, A. G., Odman, M. T., Yarwood, G., & Kumar, N. (2017). Recommendations on statistics and benchmarks to assess photochemical model performance. *Journal of the Air and Waste Management Association*, *67*(5), 582–598. https://doi.org/10.1080/10962247.2016.1265027

Gen, M., Liang, Z., Zhang, R., Go, B.R. and Chan, C.K., 2022. Particulate nitrate photolysis in the atmosphere. *Environmental Science: Atmospheres*, *2*(2), pp.111-127.

Goldberg, D.L., Anenberg, S.C., Lu, Z., Streets, D.G., Lamsal, L.N., E McDuffie, E., Smith, S.J., 2021. Urban NOx emissions around the world declined faster than anticipated between 2005 and 2019. Environ. Res. Lett. 16, 115004. https://doi.org/10.1088/1748-9326/ac2c34

Goldberg, D. L., de Foy, B., Nawaz, M. O., Johnson, J., Yarwood, G., & Judd, L. 2024a. Quantifying NOx Emission Sources in Houston, Texas Using Remote Sensing Aircraft Measurements and Source Apportionment Regression Models. *ACS ES&T Air*, *1*(11), 1391-1401.

Goldberg, D.L., Harkey, M., de Foy, B., Judd, L., Johnson, J., Yarwood, G. and Holloway, T., 2022. Evaluating NOx emissions and their effect on O3 production in Texas using TROPOMI NO_2 and HCHO. Atmospheric Chemistry and Physics, 22(16), pp.10875-10900.

Goldberg, D.L., Lu, Z., Oda, T., Lamsal, L.N., Liu, F., Griffin, D., McLinden, C.A., Krotkov, N.A., Duncan, B.N., Streets, D.G., 2019a. Exploiting OMI NO_2 satellite observations to infer fossil-fuel CO2 emissions from U.S. megacities. Sci. Total Environ. 695, 133805. https://doi.org/10.1016/j.scitotenv.2019.133805

Goldberg, D.L., Lu, Z., Streets, D.G., de Foy, B., Griffin, D., McLinden, C.A., Lamsal, L.N., Krotkov, N.A., Eskes, H.J., 2019b. Enhanced Capabilities of TROPOMI NO_2: Estimating NOx from North American Cities and Power Plants. Environ. Sci. Technol. 53, 12594–12601. https://doi.org/10.1021/acs.est.9b04488

Goldberg, D.L., Nawaz, M.O., Johnson, J., Yarwood, G., Judd, L., de Foy, B., 2023. Source-sector NOx emissions analysis with sub-kilometer scale airborne observations in Houston during TRACER-AQ AQRP Project 22-023.

Goldberg, D.L., Tao, M., Kerr, G.H., Ma, S., Tong, D.Q., Fiore, A.M., Dickens, A.F., Adelman, Z.E. and Anenberg, S.C., 2024b. Evaluating the spatial patterns of US urban NOx emissions using TROPOMI NO_2. Remote Sensing of Environment, 300, p.113917.

Harkey, M., Holloway, T., Oberman, J. and Scotty, E., 2015. An evaluation of CMAQ NO_2 using observed chemistry-meteorology correlations. Journal of Geophysical Research: Atmospheres, 120(22), pp.11-775.

Hildebrandt Ruiz, L. and Yarwood, G., 2013. Interactions between Organic Aerosol and NOy. Report prepared for the Texas AQRP (Project 12-012), available at https://aqrp.ceesa.utexas.edu/research/projects/fy-2012-2013/116-project-number-12-012 (last access 28 July 2025).

Holloway, T., Harkey, M., Kim, E., Johnson, J., Yarwood, G., Goldberg, D.L., 2021. New Satellite Tools to Evaluate Emission Inventories: Is a 3-D Model Necessary? AQRP Project 20-020.

Hudman, R.C., Moore, N.E., Mebust, A.K., Martin, R.V., Russell, A.R., Valin, L.C. and Cohen, R.C., 2012. Steps towards a mechanistic model of global soil nitric oxide emissions: implementation and space based-constraints. Atmospheric Chemistry and Physics, 12(16), pp.7779-7795.

Kemball-Cook, S., Yarwood, G., Johnson, J., Dornblaser, B. and Estes, M., 2015. Evaluating NOx emission inventories for regulatory air quality modeling using satellite and air quality model data. Atmospheric Environment, 117, pp.1-8.

Li, Y., Carlton, A.G. and Shiraiwa, M., 2021. Diurnal and seasonal variations in the phase state of secondary organic aerosol material over the contiguous US simulated in CMAQ. *ACS Earth and Space Chemistry*, *5*(8), pp.1971-1982.

Liu, S., Shilling, J.E., Song, C., Hiranuma, N., Zaveri, R.A. and Russell, L.M., 2012. Hydrolysis of organonitrate functional groups in aerosol particles. Aerosol Science and Technology, 46(12), pp.1359-1369.

Luo, C., Y. Wang, W.J. Koshak, 2017: "Development of a self-consistent lightning NOx simulation in large-scale 3-D models." J. Geophys. Res. Atmos., 122, doi:10.1002/2016JD026225.

Maclean, A.M., Li, Y., Crescenzo, G.V., Smith, N.R., Karydis, V.A., Tsimpidi, A.P., Butenhoff, C.L., Faiola, C.L., Lelieveld, J., Nizkorodov, S.A. and Shiraiwa, M., 2021. Global distribution of the phase state and mixing times within secondary organic aerosol particles in the troposphere based on room-temperature viscosity measurements. ACS Earth and Space Chemistry, 5(12), pp.3458-3473.

Murphy, D.M., Fahey, D.W., Proffitt, M.H., Liu, S.C., Chan, K.R., Eubank, C.S., Kawa, S.R. and Kelly, K.K., 1993. Reactive nitrogen and its correlation with ozone in the lower stratosphere and upper troposphere. Journal of Geophysical Research: Atmospheres, 98(D5), pp.8751-8773.

Nawaz, M. O., Johnson, J., Yarwood, G., de Foy, B., Judd, L. M., and Goldberg, D. L.: An intercomparison of satellite, airborne, and ground-level observations with WRF-CAMx simulations of NO_2 columns over Houston, TX during the September 2021 TRACER-AQ campaign, Atmospheric Chemistry and Physics, 24(11), pp.6719-6741.

Pickering, K., D. Allen, E. Bucsela, 2017: "Updates on Production of NOx by Lightning." Presented at 16th Annual CMAS Conference, Chapel Hill, NC (October 23-25, 2017).

Price, C., and D. Rind, 1992: "A simple lightning parameterization for calculating global lightning distributions." J. Geophys. Res., 97, 9919–9933, doi:10.1029/92JD00719.

Ramboll. 2025a: "Soil NOx Emission Inventory Improvements for the East Texas Council of Governments"

Ramboll. 2025b: "Soil NOx Emission Inventory Improvements for the Heart of Texas Council of Governments"

Rollins, A.W., Pusede, S., Wooldridge, P., Min, K.E., Gentner, D.R., Goldstein, A.H., Liu, S., Day, D.A., Russell, L.M., Rubitschun, C.L. and Surratt, J.D., 2013. Gas/particle partitioning of total alkyl nitrates observed with TD-LIF in Bakersfield. *Journal of Geophysical Research: Atmospheres*, *118*(12), pp.6651-6662.

Schmedding, R., Rasool, Q.Z., Zhang, Y., Pye, H.O., Zhang, H., Chen, Y., Surratt, J.D., Lopez-Hilfiker, F.D., Thornton, J.A., Goldstein, A.H. and Vizuete, W., 2020. Predicting secondary organic aerosol phase state and viscosity and its effect on multiphase chemistry in a regional-scale air quality model. *Atmospheric chemistry and physics*, *20*(13), pp.8201-8225.

Shah, V., Jacob, D.J., Dang, R., Lamsal, L.N., Strode, S.A., Steenrod, S.D., Boersma, K.F., Eastham, S.D., Fritz, T.M., Thompson, C. and Peischl, J., 2023. Nitrogen oxides in the free troposphere: implications for tropospheric oxidants and the interpretation of satellite NO_2 measurements. *Atmospheric Chemistry and Physics*, *23*(2), pp.1227-1257.

Shiraiwa, M., Li, Y., Tsimpidi, A.P., Karydis, V.A., Berkemeier, T., Pandis, S.N., Lelieveld, J., Koop, T. and Pöschl, U., 2017. Global distribution of particle phase state in atmospheric secondary organic aerosols. Nature communications, 8(1), p.15002.

Skamarock, W. C., Klemp, J. B., Dudhia, J., Gill, D. O., Barker, D. M., Wang, W., & Powers, J. G. (2005). *A Description of the Advanced Research WRF Version 2*.

Skamarock, W. C., Klemp, J. B., Dudhia, J., Gill, D. O., Barker, D. M., Duda, M. G., et al. (2008). *A Description of the Advanced Research WRF Version 3*.

Skamarock, W. C., Klemp, J. B., Dudhia, J., Gill, D. O., Liu, Z., Berner, J., et al. (2021). *A Description of the Advanced Research WRF Model Version 4*. Retrieved from https://www2.mmm.ucar.edu/wrf/users/docs/technote/v4_technote.pdf

Souri, A.H., Choi, Y., Jeon, W., Li, X., Pan, S., Diao, L. and Westenbarger, D.A., 2016. Constraining NOx emissions using satellite NO_2 measurements during 2013 DISCOVER-AQ Texas campaign. Atmospheric environment, 131, pp.371-381.

Sun, K. (2022). Derivation of Emissions from Satellite-Observed Column Amounts and Its Application to TROPOMI NO_2 and CO Observations. *Geophysical Research Letters*, e2022GL101102. https://doi.org/10.1029/2022GL101102

Travis, K.R., Jacob, D.J., Fisher, J.A., Kim, P.S., Marais, E.A., Zhu, L., Yu, K., Miller, C.C., Yantosca, R.M., Sulprizio, M.P. and Thompson, A.M., 2016. Why do models overestimate surface ozone in the Southeast United States? Atmospheric Chemistry and Physics, 16(21), pp.13561-13577

University of Houston and Ramboll. 2021. "Final Report: Ambient Monitoring for True NO_2 Near Tyler."

Wiedinmyer, C., Akagi, S. K., Yokelson, R. J., Emmons, L. K., Al-Saadi, J. A., Orlando, J. J., & Soja, A. J. (2011). The Fire INventory from NCAR (FINN): A high-resolution global model to estimate the

emissions from open burning. *Geoscientific Model Development*, *4*(3), 625–641. https://doi.org/10.5194/gmd-4-625-2011

Ye, C., Zhou, X., Pu, D., Stutz, J., Festa, J., Spolaor, M., Tsai, C., Cantrell, C., Mauldin, R.L., Campos, T. and Weinheimer, A., 2016. Rapid cycling of reactive nitrogen in the marine boundary layer. *Nature*, *532*(7600), pp.489-491.

Zhao, Q., Xie, H.B., Ma, F., Nie, W., Yan, C., Huang, D., Elm, J. and Chen, J., 2023. Mechanism-based structure-activity relationship investigation on hydrolysis kinetics of atmospheric organic nitrates. *npj Climate and Atmospheric Science*, *6*(1), p.192.